Intense Bed-Load Transport: From Laminar Bed-Load to Turbulent Sheet Flow

On the relevancy of dense granular flow rheology for bed-load transport

Julien Chauchat

LEGI CNRS - Grenoble University (julien.chauchat@grenoble-inp.fr)

18 octobre 2013

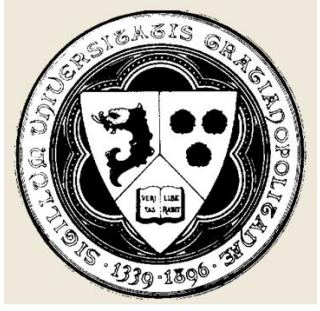

1. Introduction

2. Laminar bed-load
   - Experiments:Index-matching technique
   - Modeling approaches:Two-phase model
   - Model data comparisons

3. Sheet-flow of massive particles
   - Modeling approach
   - Validation and comparison with literature data
   - Sheet-flow experiments at LEGI

4. Conclusions and on-going work

Sediment transport

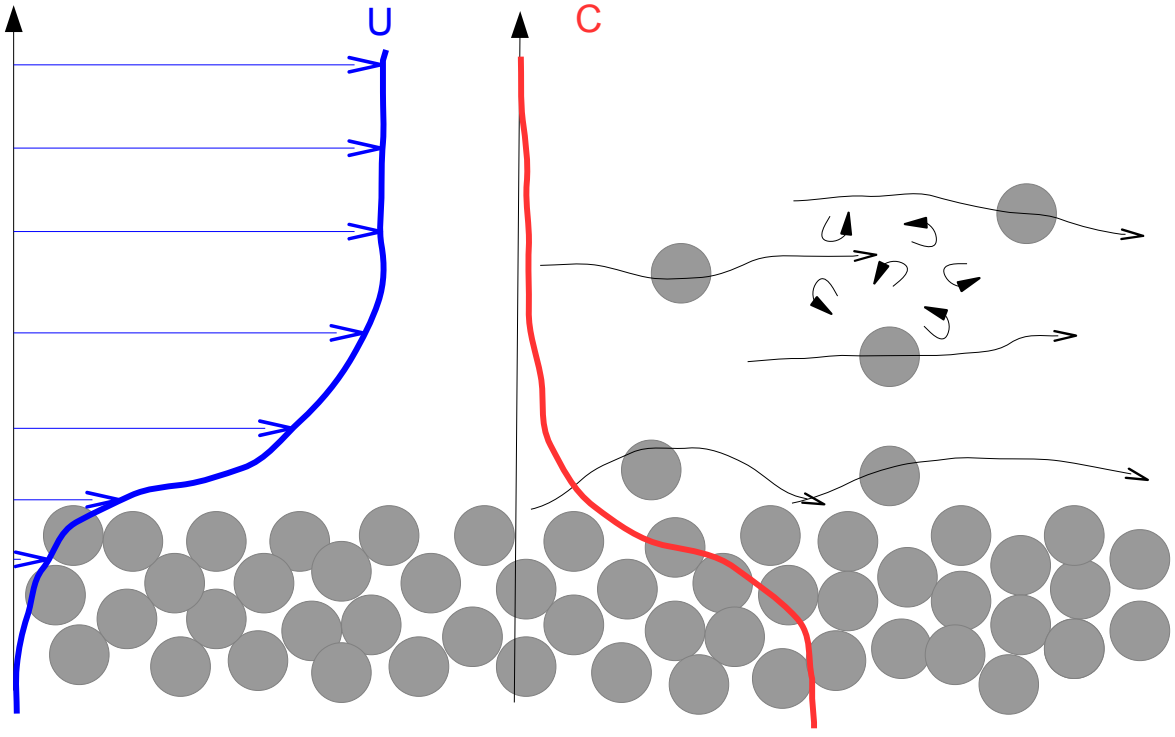

Sediment transport modes:

- **suspended-load**
particles are transported without contact with the bed.

- **bed-load**
particles are transported with intermittent or permanent contact with the bed

Suspended-load is dominated by fluid particle turbulent interactions

Bed-load is dominated by particle-particle interactions: collisions and friction

Dimensionless numbers

- **Reynolds numbers:**
  - fluid flow: $Re = \dfrac{UH}{\nu_f}$
  - particulate: $Re_p = \dfrac{w_s d_p}{\nu_f}$

U some mean flow velocity
H typical fluid flow thickness
ν_f kinematic viscosity
w_s settling velocity
d_p particle size

Dimensionless numbers

- **Reynolds numbers:**
  - fluid flow: $Re = \dfrac{UH}{\nu_f}$
  - particulate: $Re_p = \dfrac{w_s d_p}{\nu_f}$

U some mean flow velocity
H typical fluid flow thickness
ν_f kinematic viscosity
w_s settling velocity
d_p particle size

- **Shields number:** $\theta = \dfrac{\tau_f^{bed}}{\Delta\rho g d_p} = \dfrac{\rho_f u_*^2}{\Delta\rho g d_p}$

$\theta < \theta_c \Rightarrow$ No bed-load

τ_f^{bed} fluid bed shear stress
u_* friction velocity
ρ_f fluid density
ρ_s particle density
$\Delta\rho = \rho_s - \rho_f$ density difference

Dimensionless numbers

- **Reynolds numbers:**
  - fluid flow: $Re = \dfrac{UH}{\nu_f}$
  - particulate: $Re_p = \dfrac{w_s d_p}{\nu_f}$

U some mean flow velocity
H typical fluid flow thickness
ν_f kinematic viscosity
w_s settling velocity
d_p particle size

- **Shields number:** $\theta = \dfrac{\tau_f^{bed}}{\Delta\rho g d_p} = \dfrac{\rho_f u_*^2}{\Delta\rho g d_p}$

$\theta < \theta_c \Rightarrow$ No bed-load

τ_f^{bed} fluid bed shear stress
u_* friction velocity
ρ_f fluid density
ρ_s particle density
$\Delta\rho = \rho_s - \rho_f$ density difference

- **Suspension number:** $\dfrac{w_s}{u_*}$

$\dfrac{w_s}{u_*} > 1 \Rightarrow$ No suspended-load

- **Stokes number:** $St = \dfrac{\tau_p}{\tau_f}$

where τ_f: fluid timescale and τ_p: particle relaxation time scale

Observations: What happens when the Shields number is increased?

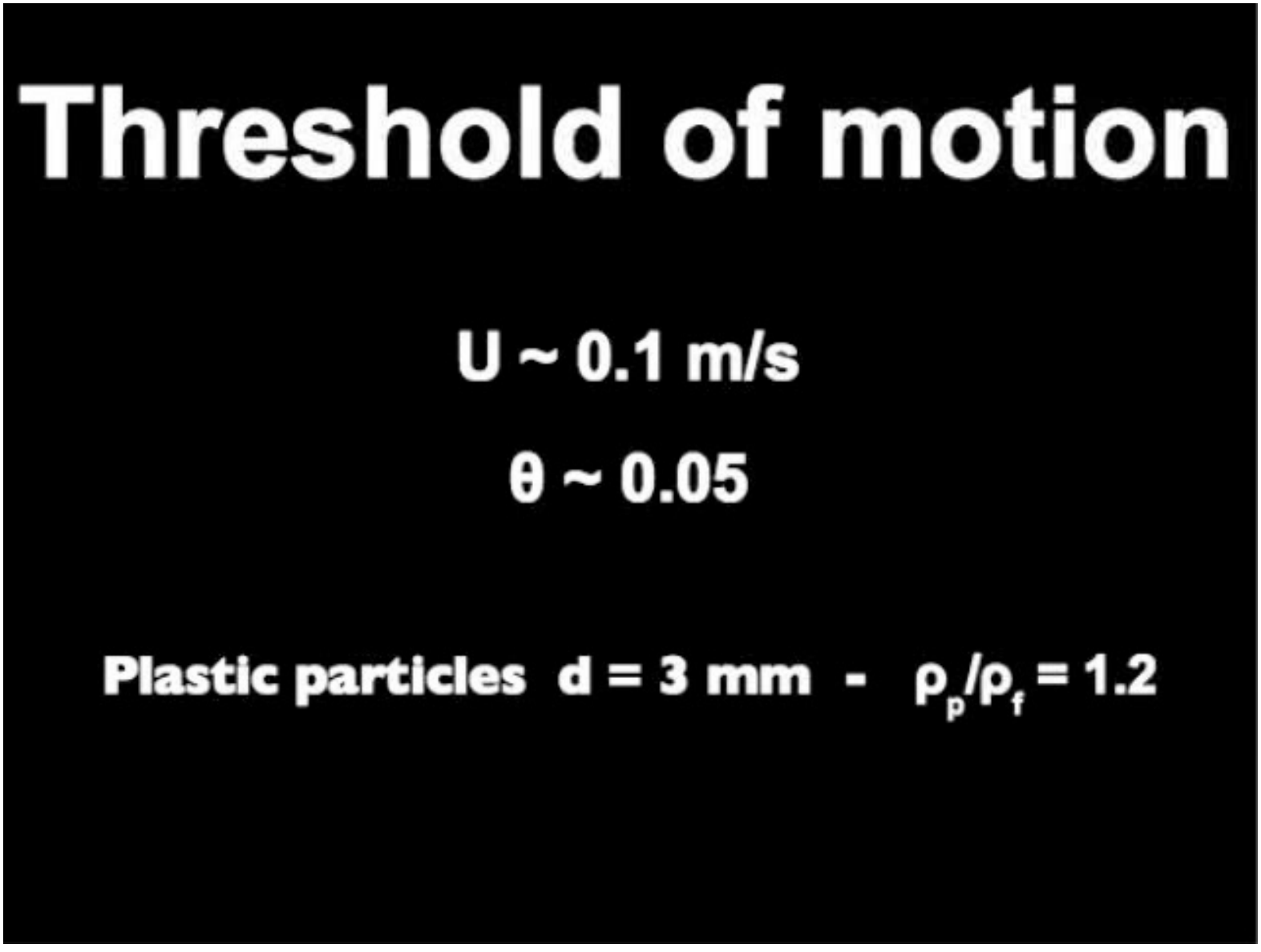

Observations: What happens when the Shields number is increased?

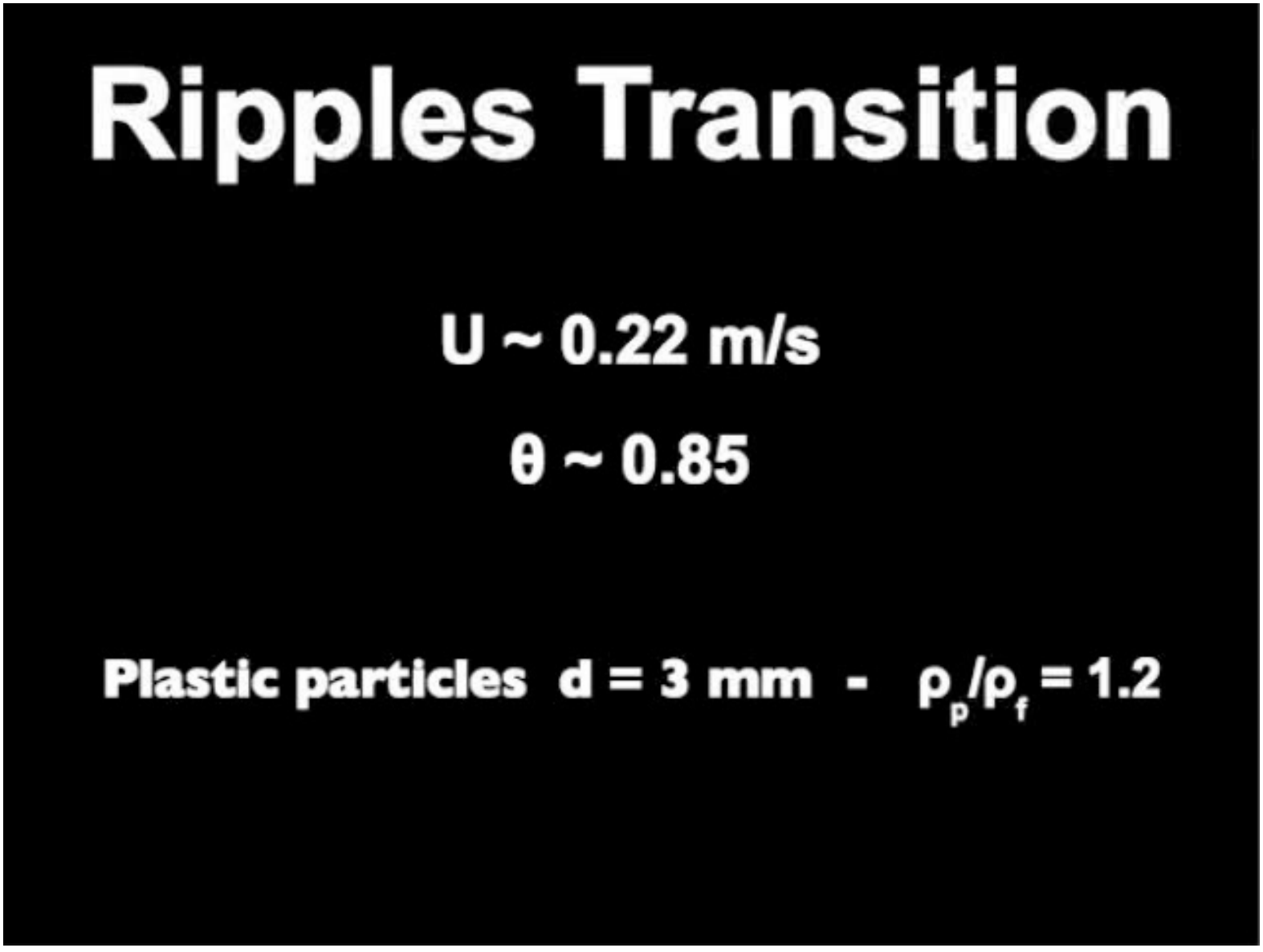

!!! $\theta \approx 0.085$!!!

Observations: What happens when the Shields number is increased?

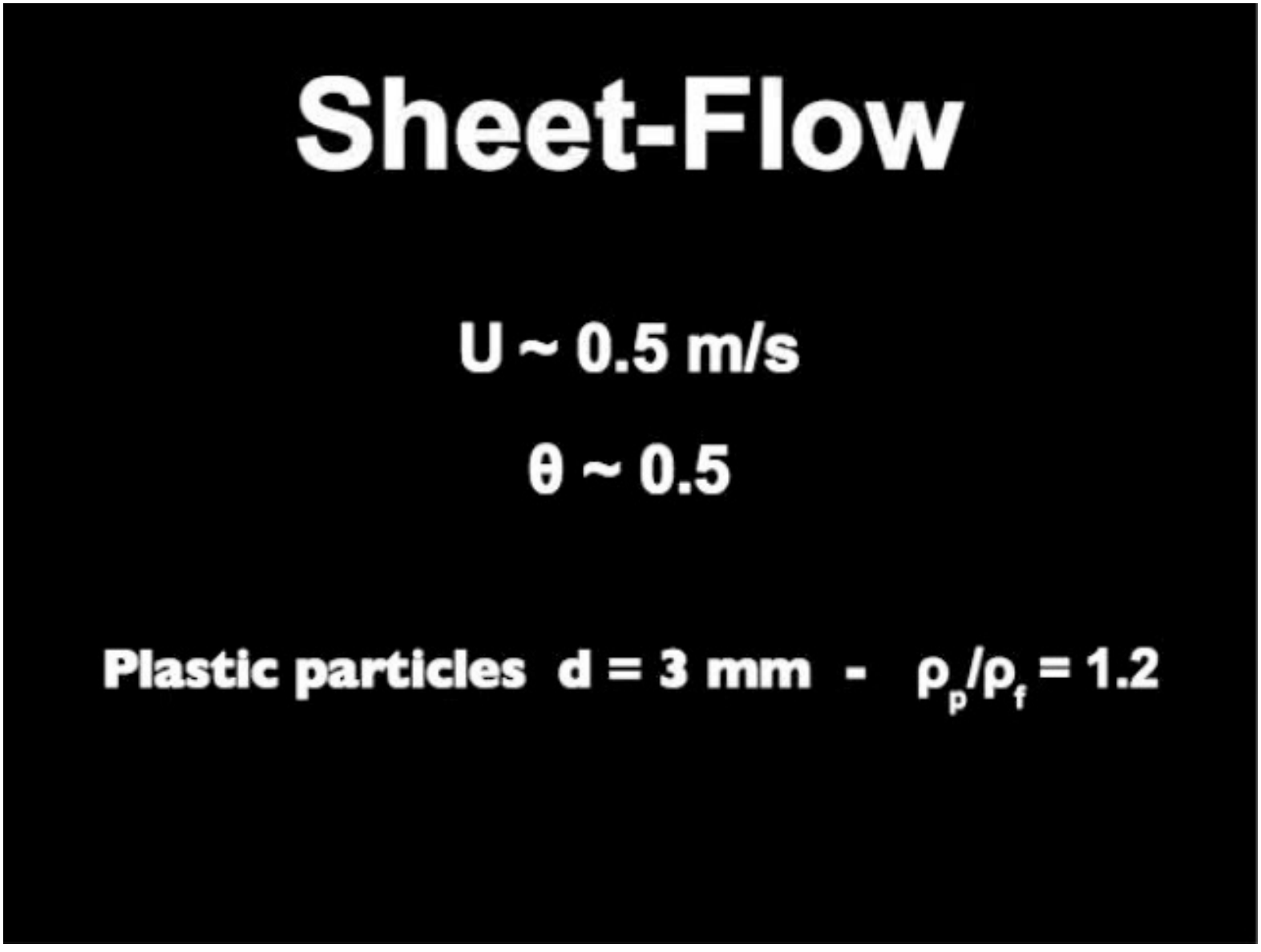

Fluid-particulate modelling approaches

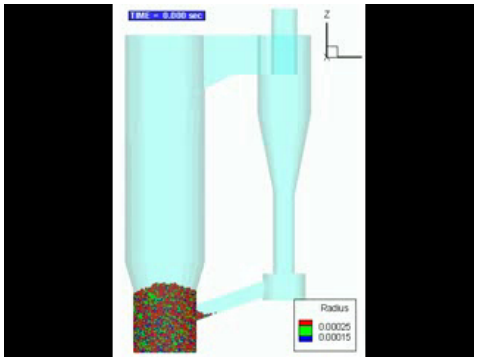

Idea 1: Eulerian - Lagrangian approach

→ Fluid flow around each particle solved explicitely
⇒ Resultant force and torque exerted on each particle

→ Particle-particle interactions explicitely solved

→ Limited to small number of particles

"DNS at the particle scale" ($\geq$2000's)

Fluid-particulate modelling approaches

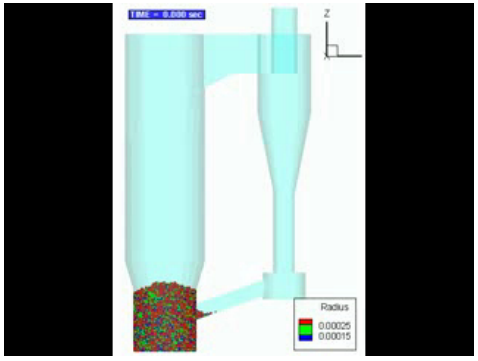

Idea 1: Eulerian - Lagrangian approach

→ Fluid flow around each particle solved explicitely
⇒ Resultant force and torque exerted on each particle

→ Particle-particle interactions explicitely solved

→ Limited to small number of particles

"DNS at the particle scale" ($\geq$2000's)

Idea 2: Eulerian - Lagrangian approach

→ Fluid velocity spatially averaged $V_{average} >> V_{particle}$
⇒ $F_{fluid \rightarrow particle} = f(\phi, \overrightarrow{u_r})$ empirical correlations

→ Particle-particle interactions explicitely solved

"Discrete Particle Modelling" ($\geq$1990's)

Fluid-particulate modelling approaches

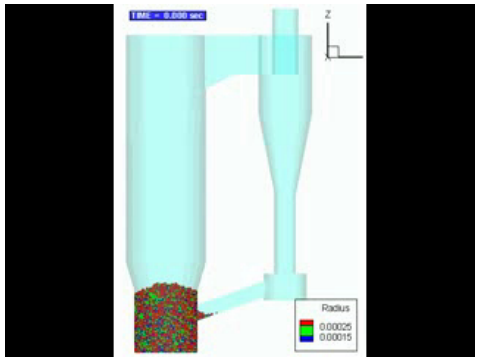

Idea 1: Eulerian - Lagrangian approach

→ Fluid flow around each particle solved explicitely

⇒ Resultant force and torque exerted on each particle

→ Particle-particle interactions explicitely solved

→ Limited to small number of particles

"DNS at the particle scale" ($\geq$2000's)

Idea 2: Eulerian - Lagrangian approach

→ Fluid velocity spatially averaged $V_{average} >> V_{particle}$

⇒ $F_{fluid \rightarrow particle} = f(\phi, \overrightarrow{u_r})$ empirical correlations

→ Particle-particle interactions explicitely solved

"Discrete Particle Modelling" ($\geq$1990's)

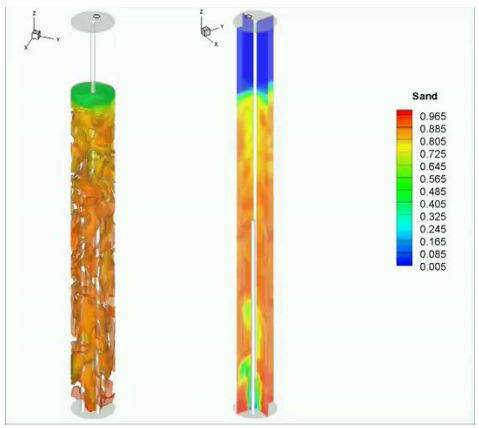

Idea 3: Eulerian - Eulerian approach

→ Fluid and particles velocities spatially averaged

$V_{average} >> V_{particle}$

⇒ $F_{fluid \rightarrow particle} = f(\phi, \overrightarrow{u_r})$ empirical correlations

→ No limitation on the number of particles

"Two-fluid model"

2 arguments for an Eulerian approach

- How much particles of 1 mm diameter in a cube of 10 cm side filled at 60% ?

$$With \begin{cases} d_p = 10^{-3}\ m \\ L = 10^{-1}\ m \\ \phi = 0.6 \end{cases} \qquad we\ get \begin{cases} V_t = L^3 = 10^{-3}\ m^3 \\ v_p = \frac{\pi}{6} d_p^3 \approx 5.10^{-10}\ m^3 \\ N_p = \frac{\phi V_t}{v_p} \approx 10^6\ particles \end{cases}$$

$\longrightarrow$ Impossible to solve all the fluid scales and all the particles motion in dense systems. There is a need for some upscaling !

2 arguments for an Eulerian approach

- How much particles of 1 mm diameter in a cube of 10 cm side filled at 60% ?

$$With \begin{cases} d_p = 10^{-3}\ m \\ L = 10^{-1}\ m \\ \phi = 0.6 \end{cases} \qquad we\ get \begin{cases} V_t = L^3 = 10^{-3}\ m^3 \\ v_p = \frac{\pi}{6} d_p^3 \approx 5.10^{-10}\ m^3 \\ N_p = \frac{\phi V_t}{v_p} \approx 10^6\ particles \end{cases}$$

$\longrightarrow$ Impossible to solve all the fluid scales and all the particles motion in dense systems. There is a need for some upscaling !

- The solution of the Lagrangian model *would provide more detailed information than it is usually needed. Indeed, a knowledge of the average values of the velocity of the fluid, the velocities and angular velocities of the particles, and the fluid pressure, over some appropriately small region in the neighbourhood of each point [...], is usually all that is required.*

Jackson (1997)

$\Rightarrow$ **Eulerian - Eulerian approach** (Idea 3)

Two-phase "two-fluid" equations

$$\begin{cases} \epsilon, \phi & : \text{Volume fractions} \\ \overrightarrow{u^f}, \overrightarrow{u^p} & : \text{Average velocities} \\ n\overrightarrow{f} & : \text{Force fluid} \leftrightarrow \text{particle} \end{cases}$$

- **Continuity equations**

$$\frac{\partial \epsilon}{\partial t} + \overrightarrow{\nabla}.\left(\epsilon \overrightarrow{u^f}\right) = 0 \qquad \frac{\partial \phi}{\partial t} + \overrightarrow{\nabla}.\left(\phi \overrightarrow{u^p}\right) = 0 \qquad \phi + \epsilon = 1$$

- **Momentum equations**

$$\rho_f \left[\frac{\partial \epsilon \overrightarrow{u^f}}{\partial t} + \overrightarrow{\nabla}.\left(\epsilon \overrightarrow{u^f} \otimes \overrightarrow{u^f}\right)\right] = -\overrightarrow{\nabla} p^f + \overrightarrow{\nabla}.\left(\overline{\overline{\tau^f}}\right) - n\overrightarrow{f} + \epsilon \rho_f \overrightarrow{g}$$

$$\underbrace{\rho_p \left[\frac{\partial \phi \overrightarrow{u^p}}{\partial t} + \overrightarrow{\nabla}.\left(\phi \overrightarrow{u^p} \otimes \overrightarrow{u^p}\right)\right]}_{Inertia} = \underbrace{-\overrightarrow{\nabla} p^p + \overrightarrow{\nabla}.\left(\overline{\overline{\tau^p}}\right)}_{Stresses} + \underbrace{n\overrightarrow{f}}_{Interaction} + \underbrace{\phi \rho_p \overrightarrow{g}}_{Gravity}$$

Closure issue: relate the fluid and particulate phase stress tensors $\overline{\overline{\sigma^f}} = -p^f \overline{\overline{I}} + \overline{\overline{\tau^f}}$, $\overline{\overline{\sigma^p}} = -p^p \overline{\overline{I}} + \overline{\overline{\tau^p}}$ and the interaction term $n\overrightarrow{f}$ to the average variables $\epsilon, \phi, \overrightarrow{u^f}, \overrightarrow{u^p}$

Remark: The mixture is incompressible $\overrightarrow{\nabla}.\left(\phi \overrightarrow{u^p} + \epsilon \overrightarrow{u^f}\right) = 0$

Closure for the particulate stress tensors : Particle-particle interactions

General stress-shear rate relationship $\boxed{\overline{\overline{\sigma^p}} = -p^p \overline{\overline{I}} + \eta^p \left(\vec{\nabla} \vec{u^p} + \vec{\nabla} \vec{u^p}^T \right)}$

where p^p and η^p depends on the physic at work

- **In very dilute suspension ($\phi \in [0.; \approx 10^{-3}?]$)**: $\overline{\overline{\sigma^p}} \approx 0$

  $\rightarrow$ No contact between particles $\Rightarrow$ no stress transmission

Closure for the particulate stress tensors : Particle-particle interactions

General stress-shear rate relationship $\boxed{\overline{\overline{\sigma^p}} = -p^p \overline{\overline{I}} + \eta^p \left(\vec{\nabla} \vec{u^p} + \vec{\nabla} \vec{u^p}^T \right)}$

where p^p and η^p depends on the physic at work

- **In very dilute suspension ($\phi \in [0.; \approx 10^{-3}?]$)**: $\overline{\overline{\sigma^p}} \approx 0$

  $\rightarrow$ No contact between particles $\Rightarrow$ no stress transmission

- **Intermediate concentration ($\phi \in [\approx 10^{-3}?; \approx 0.55?]$)**: $\overline{\overline{\sigma^p}} \neq 0$

  $\rightarrow$ Collisions between particles occurs $\Rightarrow$ collisional stresses

  $\Rightarrow$ $\boxed{p^p = p^p(\phi, T^p) \text{ and } \eta^p = \eta^p(\phi, T^p)}$ with T^p is the "granular temperature"

  Haff (1983), Jenkins and Savage (1983), Lun et al. (1984), ...

Closure for the particulate stress tensors : Particle-particle interactions

General stress-shear rate relationship $\boxed{\overline{\overline{\sigma^p}} = -p^p \overline{\overline{I}} + \eta^p \left(\vec{\nabla}\vec{u^p} + \vec{\nabla}\vec{u^p}^T \right)}$

where p^p and η^p depends on the physic at work

- **In very dilute suspension ($\phi \in [0.; \approx 10^{-3}?]$)**: $\overline{\overline{\sigma^p}} \approx 0$

  $\rightarrow$ No contact between particles $\Rightarrow$ no stress transmission

- **Intermediate concentration ($\phi \in [\approx 10^{-3}?; \approx 0.55?]$)**: $\overline{\overline{\sigma^p}} \neq 0$

  $\rightarrow$ Collisions between particles occurs $\Rightarrow$ collisional stresses

  $\Rightarrow$ $\boxed{p^p = p^p(\phi, T^p) \text{ and } \eta^p = \eta^p(\phi, T^p)}$ with T^p is the "granular temperature"

  Haff (1983), Jenkins and Savage (1983), Lun et al. (1984), ...

- **Dense systems ($\phi \in [0.3; \phi_{max}]$)**: $\overline{\overline{\sigma^p}} \neq 0$

  $\rightarrow$ Enduring contact between particles exists $\Rightarrow$ Frictional and collisional stresses

Dense granular rheology $\mu(I)$ (inertial regime)

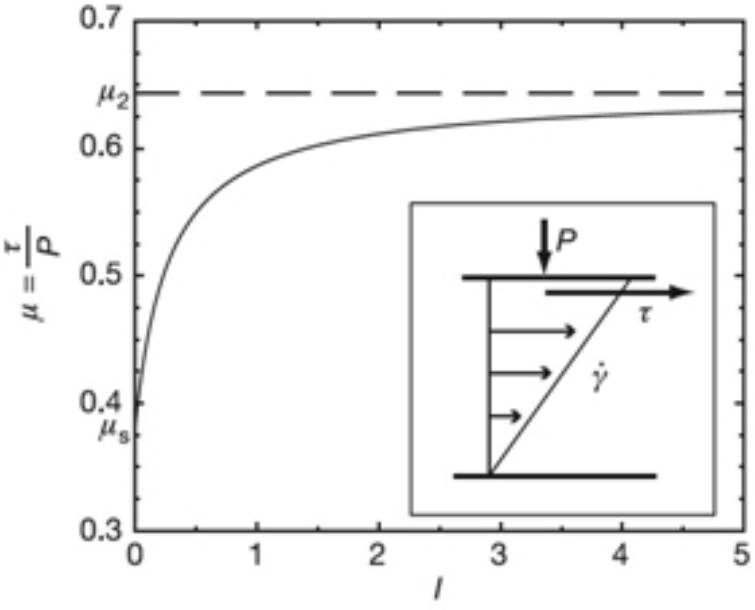

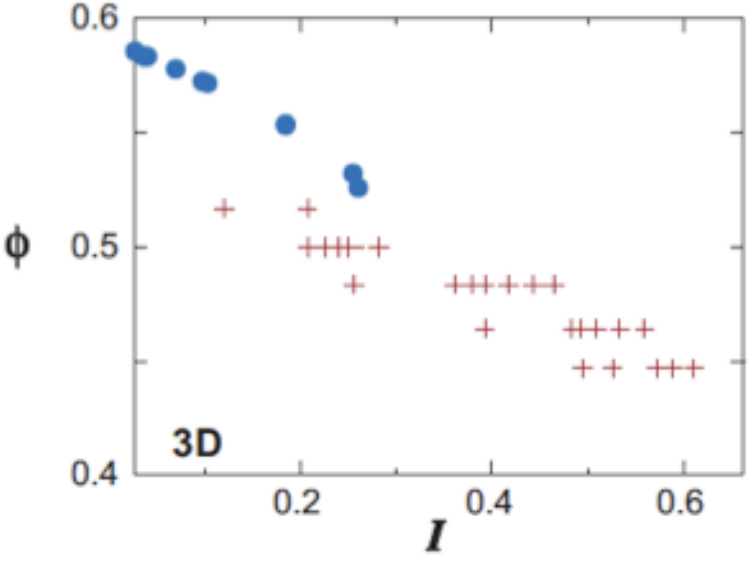

Dimensional analysis

$\Rightarrow$ Inertial parameter: $I = \dfrac{\left|\dot{\gamma}^p\right| \; d_p}{\sqrt{p^p/\rho_p}} = \dfrac{t_{micro}}{t_{macro}}$

Frictional rheology: $\boxed{\tau^p = \mu(I) \; p^p}$

$\rightarrow$ *GDR Midi (2004), Jop et al. (2006), Forterre and Pouliquen (2008)*

Dense granular rheology $\mu(I)$ (inertial regime)

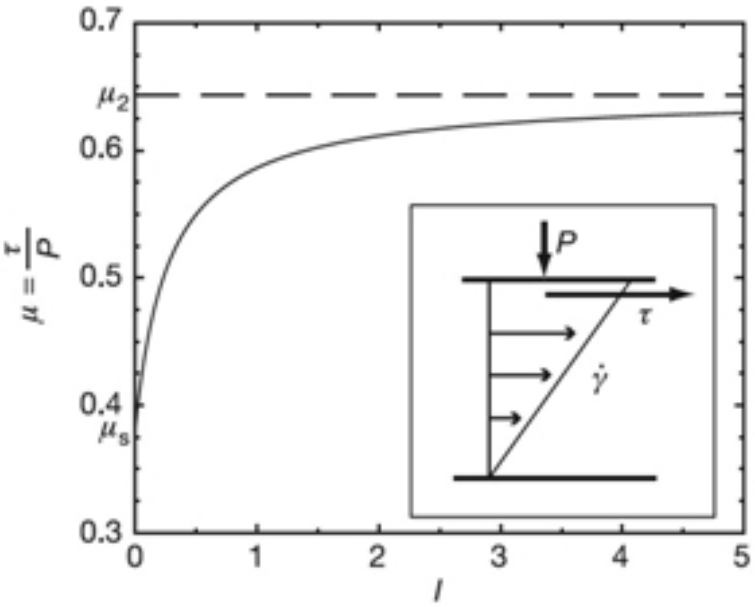

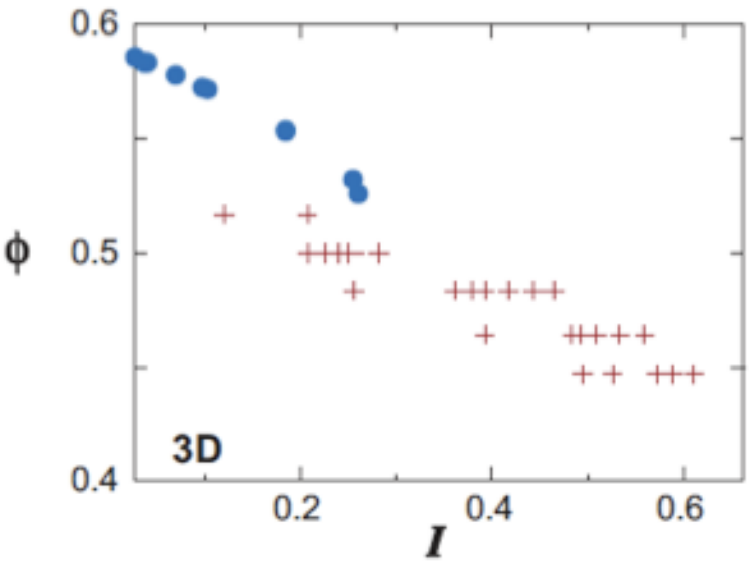

Dimensional analysis

$\Rightarrow$ Inertial parameter: $I = \dfrac{\left|\dot{\gamma}^p\right| \; d_p}{\sqrt{p^p/\rho_p}} = \dfrac{t_{micro}}{t_{macro}}$

Frictional rheology: $\boxed{\tau^p = \mu(I) \; p^p}$

$\rightarrow$ *GDR Midi (2004), Jop et al. (2006), Forterre and Pouliquen (2008)*

with $\mu(I) = \mu_s + \dfrac{\mu_2 - \mu_s}{\dfrac{I_0}{I} + 1}$

with typical values for monodisperse beads:

$$\mu_s = 0.38 \; ; \; \mu_2 = 0.65 \; ; \; I_0 = 0.3$$

Simplified frictional rheology (Coulomb):
$\rightarrow \mu = \mu_s = constant$

Dilatancy law: $\phi(I) = \phi_{max} + (\phi_{min} - \phi_{max}) \; I$

$\phi_{max} = 0.6 \; ; \; \phi_{min} = 0.4$

See Olivier Pouliquen's talk during this workshop for details

Dense granular rheology $\mu(I_v)$ (viscous regime)

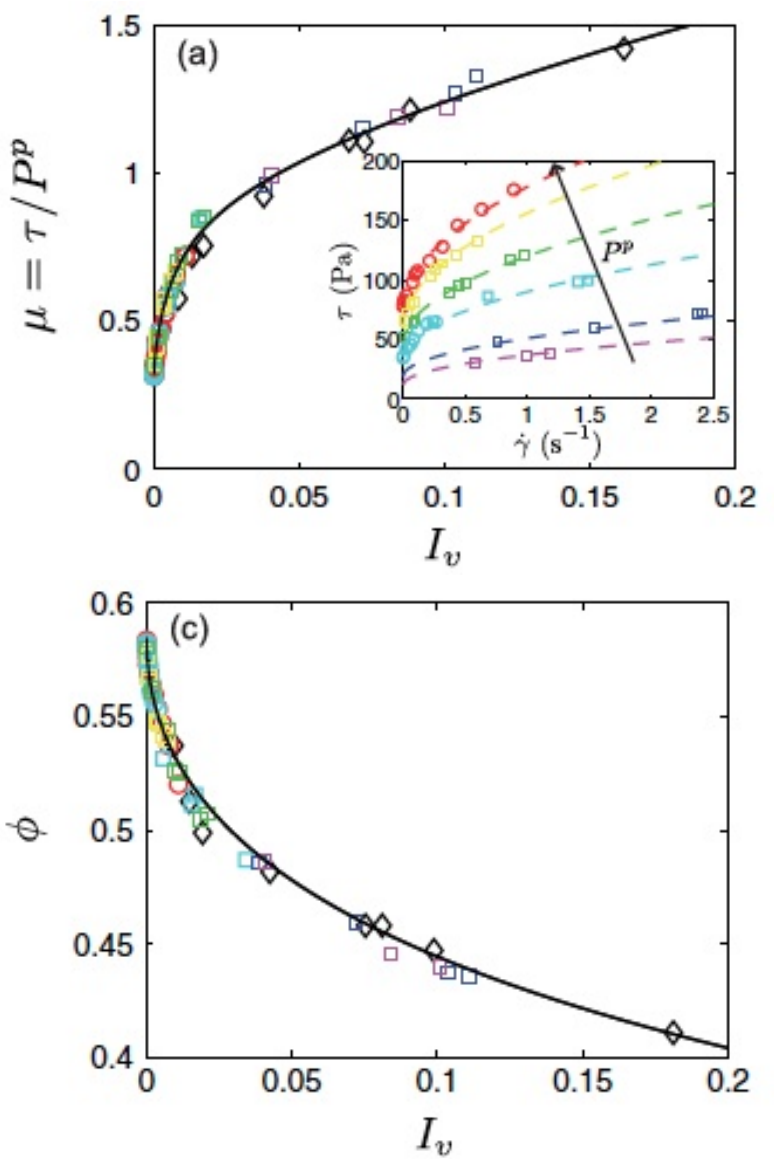

Boyer et al. (2011)

If $t_{micro}^{viscous} = \dfrac{\eta_f}{p^p} >> t_{micro}^{inertial} = \dfrac{d}{\sqrt{p^p \ / \ \rho_p}}$

Then control parameter: $I_v = \dfrac{\eta_f \, |\dot{\gamma}|}{p^p}$

From pressure-imposed rheometry measurements:

$$\mu(I_v) = \mu_s + \frac{\mu_2 - \mu_s}{I_0/I_v + 1} + I_v + \frac{5}{2}\phi_{max} I_v^{1/2}$$

$$\phi(I_v) = \frac{\phi_{max}}{1 + I_v^{1/2}}$$

That can be recasted as follows:

$$\mu^c(I_v) = \mu_s + \frac{\mu_2 - \mu_s}{I_0/I_v + 1}$$

$$\frac{\eta_e}{\eta_f} = 1 + \frac{5}{2}\phi\left(1 - \frac{\phi}{\phi_{max}}\right)^{-1}$$

with typical values for monodisperse beads in neutrally buoyant conditions:

$\mu_s = 0.32$; $\mu_2 = 0.7$; $I_0 = 0.005$; $\phi_{max} = 0.585$

Tensorial formulation of the local rheology

For 3D configurations the granular media can be sheared in different directions. Therefore a generalisation of the scalar constitutive laws to a tensorial formulation is required:

$$\overline{\overline{\sigma^p}} = -p^p \, \overline{\overline{I}} + \overline{\overline{\tau^p}},$$

where p^p is the isotropic pressure and $\boxed{\overline{\overline{\tau^p}} = \mu(I) \; p^p \frac{\overline{\overline{\dot{\gamma}^p}}}{\| \overline{\overline{\dot{\gamma}^p}} \|}}$ is the shear stress tensor.

Hypothesis and consequence:

- These relationships are based on the assumption that the shear stress tensor $\overline{\overline{\tau^p}}$ is colinear to the shear rate tensor $\overline{\overline{\dot{\gamma}^p}}$.
- One can define an effective viscosity such that: $\overline{\overline{\tau^p}} = \eta^p \overline{\overline{\dot{\gamma}^p}}$

$$\eta^p = \frac{\mu(I) \; p^p}{\| \overline{\overline{\dot{\gamma}^p}} \|}$$

Jop, Forterre and Pouliquen (2006)

Link with classical visco-plasticity

Bingham constitutive relationship

$$\begin{cases} \text{if} \quad \| \overline{\overline{\tau}} \| \leq \tau_0 \quad \text{then} \quad \overline{\overline{\dot{\gamma}}} = \overline{\overline{0}} \\ \\ \text{else} \quad \overline{\overline{\tau}} = \eta_b \, \overline{\overline{\dot{\gamma}}} \end{cases}$$

with : $\boxed{\eta_b = \eta + \dfrac{\tau_0}{\| \overline{\overline{\dot{\gamma}}} \|}}$

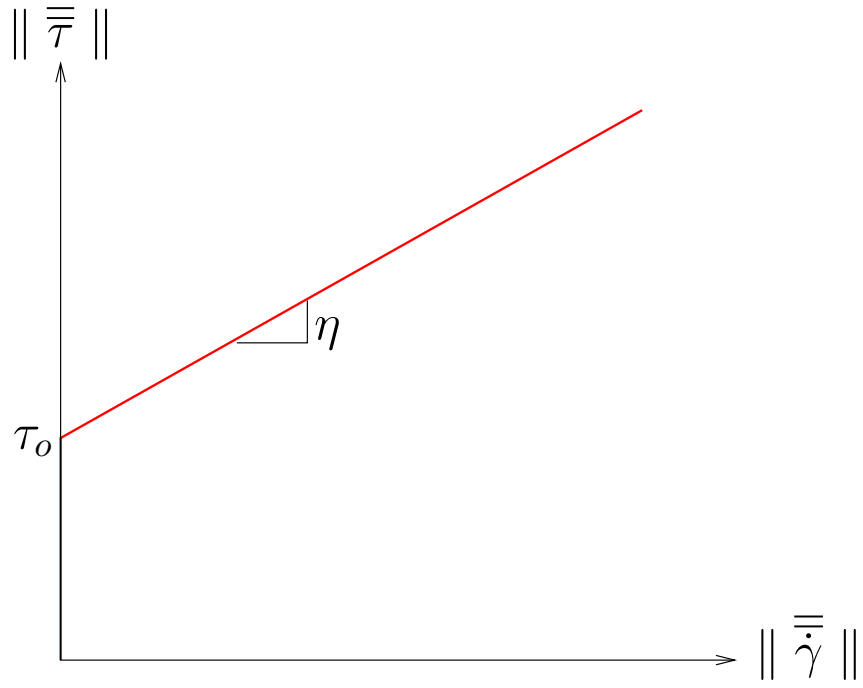

Link with classical visco-plasticity

Bingham constitutive relationship

$$\begin{cases} \text{if} \quad \| \overline{\overline{\tau}} \| \leq \tau_0 \quad \text{then} \quad \overline{\overline{\dot{\gamma}}} = \overline{\overline{0}} \\ \\ \text{else} \quad \overline{\overline{\tau}} = \eta_b \, \overline{\overline{\dot{\gamma}}} \end{cases}$$

with : $\boxed{\eta_b = \eta + \dfrac{\tau_0}{\| \overline{\overline{\dot{\gamma}}} \|}}$

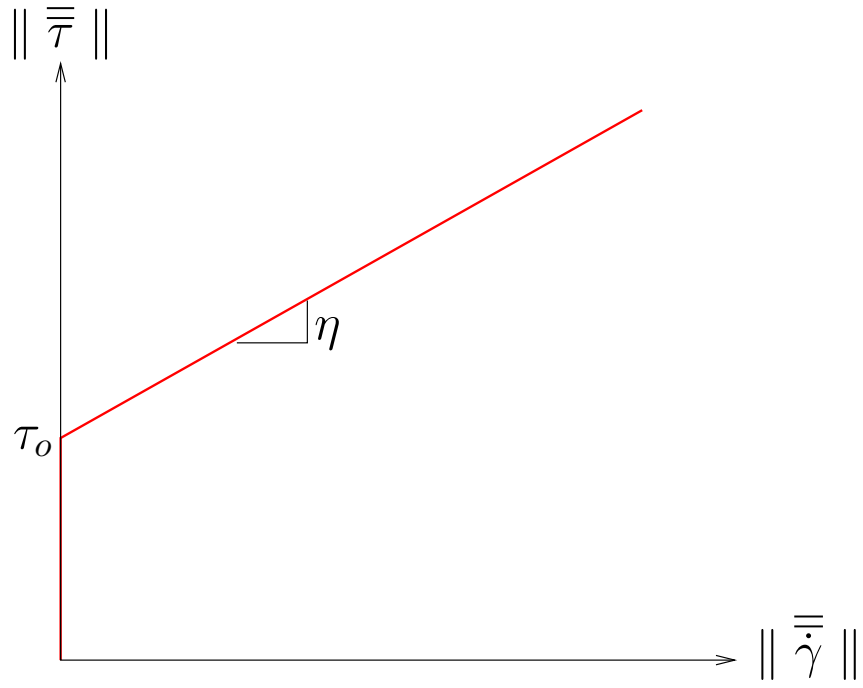

Coulomb rheology: $\mu(I) = \mu_s$

$$\overline{\overline{\tau^p}} = \mu_s \; p^p \frac{\overline{\overline{\dot{\gamma}^p}}}{\| \overline{\overline{\dot{\gamma}^p}} \|} \qquad \Longrightarrow \qquad \boxed{\eta^p = \frac{\mu_s \; p^p}{\| \overline{\overline{\dot{\gamma}^p}} \|}}$$

$\Longleftrightarrow$ Purely plastic material: $\boxed{\eta = 0}$ and $\boxed{\tau_0 = \mu_s \; p^p}$

Link with classical visco-plasticity

Bingham constitutive relationship

$$\begin{cases} \text{if} \quad \| \overline{\overline{\tau}} \| \leq \tau_0 \quad \text{then} \quad \overline{\overline{\dot{\gamma}}} = \overline{\overline{0}} \\ \\ \text{telse} \quad \overline{\overline{\tau}} = \eta_b \, \overline{\overline{\dot{\gamma}}} \end{cases}$$

with : $\boxed{\eta_b = \eta + \dfrac{\tau_0}{\| \overline{\overline{\dot{\gamma}}} \|}}$

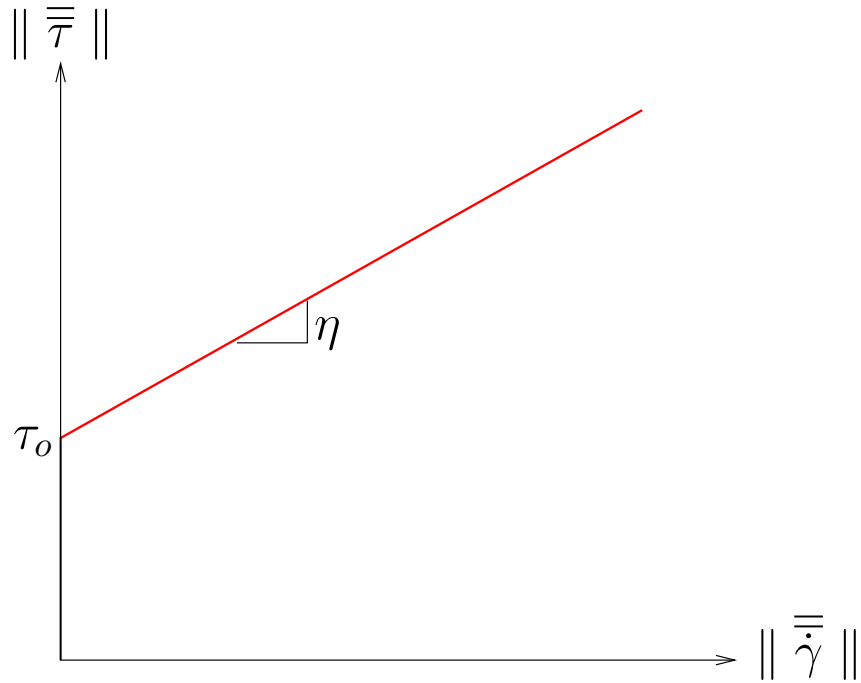

$\mu(I)$ **granular rheology:** $\mu(I) = \mu_s + \dfrac{\mu_2 - \mu_s}{I_0/I + 1}$ with $I = \dfrac{\| \overline{\overline{\dot{\gamma}^p}} \|}{f(p^p,...)}$

$$\overline{\overline{\tau^p}} = \mu(I) \; p^p \frac{\overline{\overline{\dot{\gamma}}}}{\| \overline{\overline{\dot{\gamma}^p}} \|} \qquad \Longrightarrow \qquad \boxed{\eta^p = \frac{\mu_s \; p^p}{\| \overline{\overline{\dot{\gamma}^p}} \|} + \frac{(\mu_2 - \mu_s) \; p^p}{I_0 \; f(p^p,...) + \| \overline{\overline{\dot{\gamma}^p}} \|}}$$

$\Longleftrightarrow$ visco-plastic material $\boxed{\eta(\overline{\overline{\dot{\gamma}^p}}) = \dfrac{(\mu_2 - \mu_s) \; p^p}{I_0 f(p^p,...) + \| \overline{\overline{\dot{\gamma}^p}} \|}}$ and $\boxed{\tau_0 = \mu_s \; p^p}$

$\rightarrow$ non-conventional shear thinning rheology

Numerical methods for visco-plastic flows

Two main approaches:

- **Regularization methods**
- Multipliers methods $\rightarrow$ *e.g.* Augmented Lagrangian Method

[Dean, Glowinsky and Guidoboni, 2007]

Regularization: $\eta_b = \eta + \dfrac{\tau_0}{\| \overline{\overline{\dot{\gamma}}} \|}$

- Issue: η_b diverges when $\| \overline{\overline{\dot{\gamma}}} \| \longrightarrow 0$
- Simplest solution: viscosity regularization (Frigaard and Nouar, 2005)

$$\textit{i.e. } \eta_b = \eta + \frac{\tau_0}{\| \overline{\overline{\dot{\gamma}}} \| + \lambda} \text{ with } \lambda \text{ small numerical parameter}$$

Numerical methods for visco-plastic flows

Two main approaches:

- **Regularization methods**
- Multipliers methods $\rightarrow$ *e.g.* Augmented Lagrangian Method

[Dean, Glowinsky and Guidoboni, 2007]

Regularization: $\eta_b = \eta + \dfrac{\tau_0}{\| \overline{\overline{\dot{\gamma}}} \|}$

- Issue: η_b diverges when $\| \overline{\overline{\dot{\gamma}}} \| \longrightarrow 0$
- Simplest solution: viscosity regularization (Frigaard and Nouar, 2005)

$$\textit{i.e. } \eta_b = \eta + \frac{\tau_0}{\| \overline{\overline{\dot{\gamma}}} \| + \lambda} \text{ with } \lambda \text{ small numerical parameter}$$

Regularisation of the $\mu(I)$ rheology

$$\eta^p_{mc} = \left[\mu_s + \frac{(\mu_2 - \mu_s) \| \overline{\overline{\dot{\gamma}^p}} \|}{I_0 f(p^p,...) + \| \overline{\overline{\dot{\gamma}^p}} \|} \right] \frac{p^p}{\left(\| \overline{\overline{\dot{\gamma}^p}} \|^2 + \lambda^2 \right)^{1/2}}$$

see Chauchat and Medale (2010, 2013)

1. Introduction

2. Laminar bed-load
   - Experiments:Index-matching technique
   - Modeling approaches:Two-phase model
   - Model data comparisons

3. Sheet-flow of massive particles
   - Modeling approach
   - Validation and comparison with literature data
   - Sheet-flow experiments at LEGI

4. Conclusions and on-going work

This work has been done in collaboration with **Pascale Aussillous**, Elizabeth Guazzelli, Marc Médale and Mickael Pailha at the IUSTI Lab in Marseille (France).

1. Introduction

2. Laminar bed-load
   - Experiments:Index-matching technique
   - Modeling approaches:Two-phase model
   - Model data comparisons

3. Sheet-flow of massive particles
   - Modeling approach
   - Validation and comparison with literature data
   - Sheet-flow experiments at LEGI

4. Conclusions and on-going work

Experimental set-up

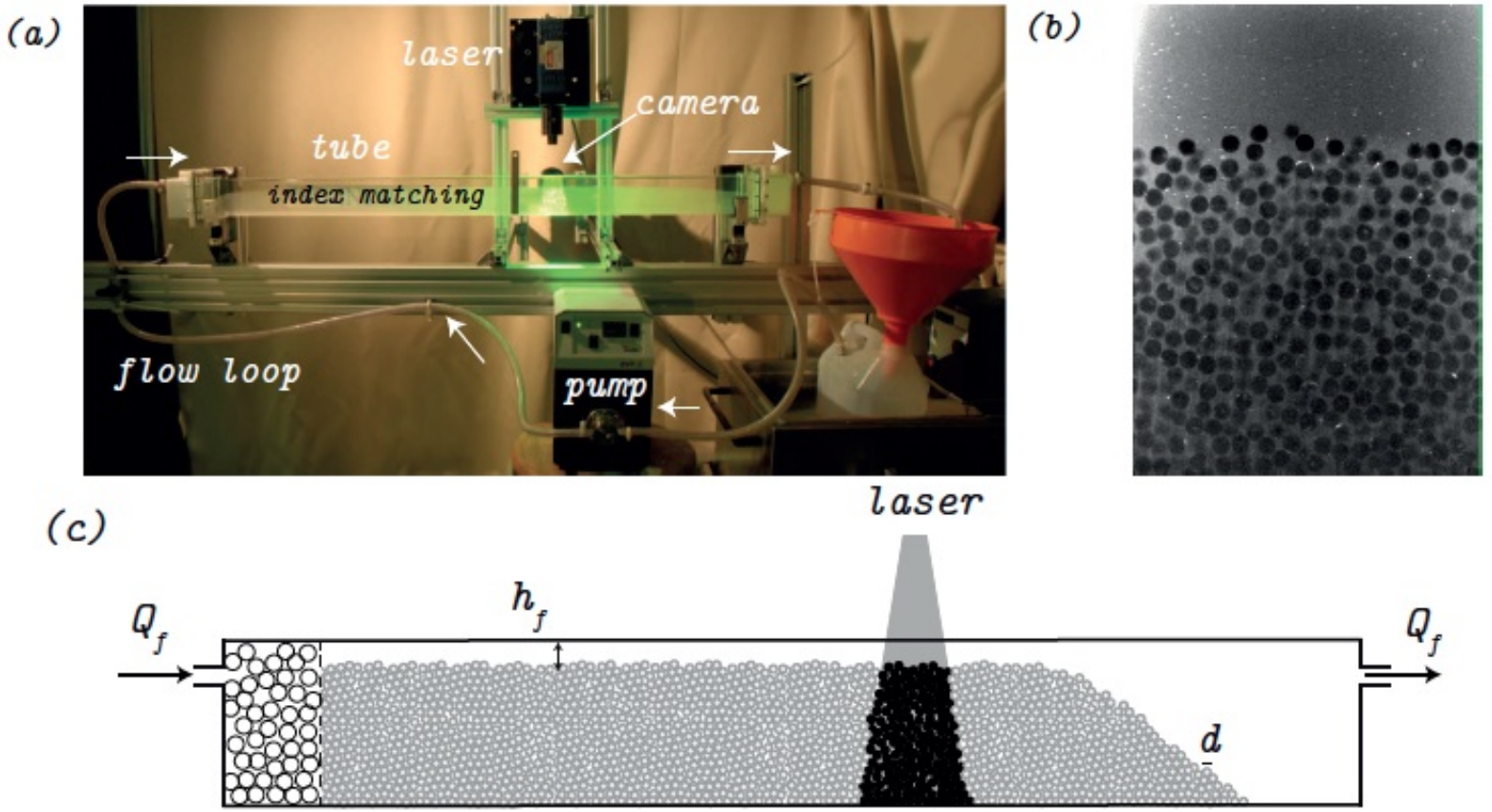

- H = 6.5 cm
- W = 3.5 cm
- L = 100 cm

- Laser 2000, 532 nm, 100 mW
- digital camera (Basler Scout): 1392x1040 ; 20 fps
- dye: Rhodamine 6G fluoresces at λ >555 nm
- fluid tracers: Finger print powder (white dots)

Borosilicate: $d_p = 1.1$mm ; $\rho_p = 2230$kg.m^{-3} ; $\rho_f = 1060$kg.m^{-3} ; $\eta_f = 320\ 10^{-3}$Pa.s

PMMA: $d_p = 2.04$mm ; $\rho_p = 1190$kg.m^{-3} ; $\rho_f = 1070$kg.m^{-3} ; $\eta_f = 270\ 10^{-3}$Pa.s

Experiments: Index-matching technique

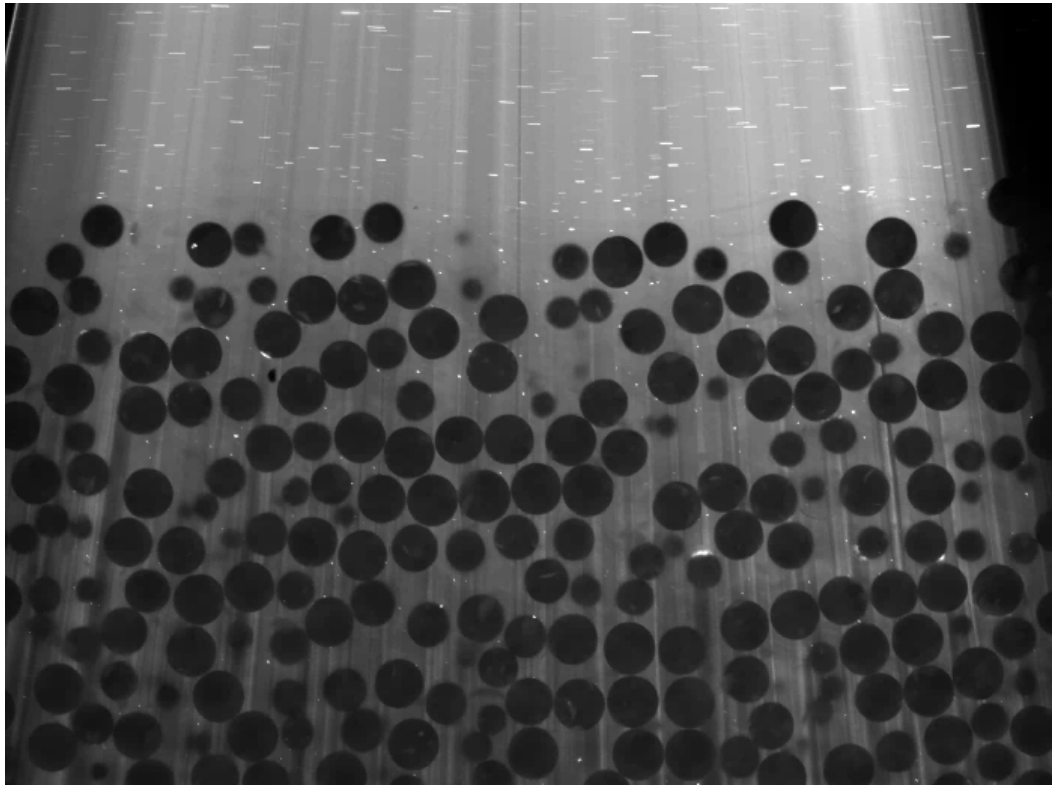

- Laminar viscous regime: $Re \in [0.2; 1.2]$
- Mobile dense granular medium $\phi \approx 0.55$ (constant)

$\Rightarrow$ Intense bed-load: $\theta >> \theta_c$ with $\theta \in [0.2; 1.2]$ and $\theta_c = 0.12$

Thickness of the layer $>$ particle size

Bed interface tracking

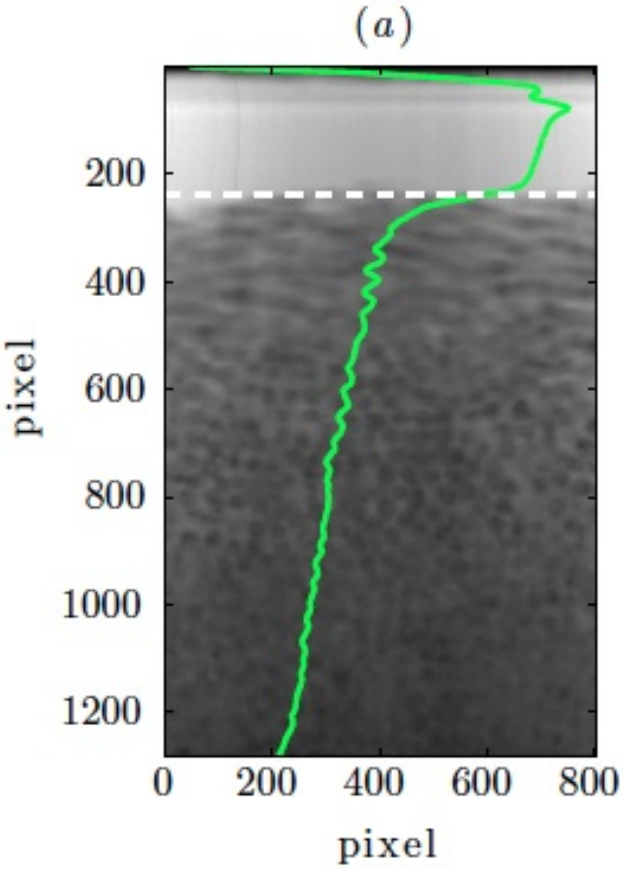

Grey level

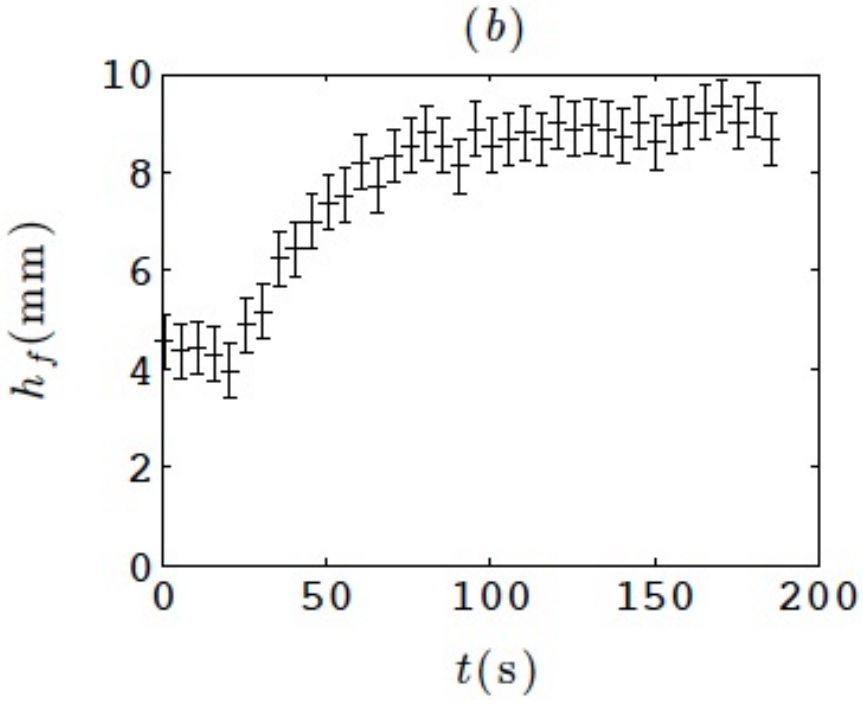

Fluid bed interface as function of time

h_f is deduced from a threshold criteria on the average grey level profile (over 10 frames)

$h_f(t)$ is measured every 5 s

Initial decrease of h_f is due to dilatation of the granular layer

Velocity and concentration profiles

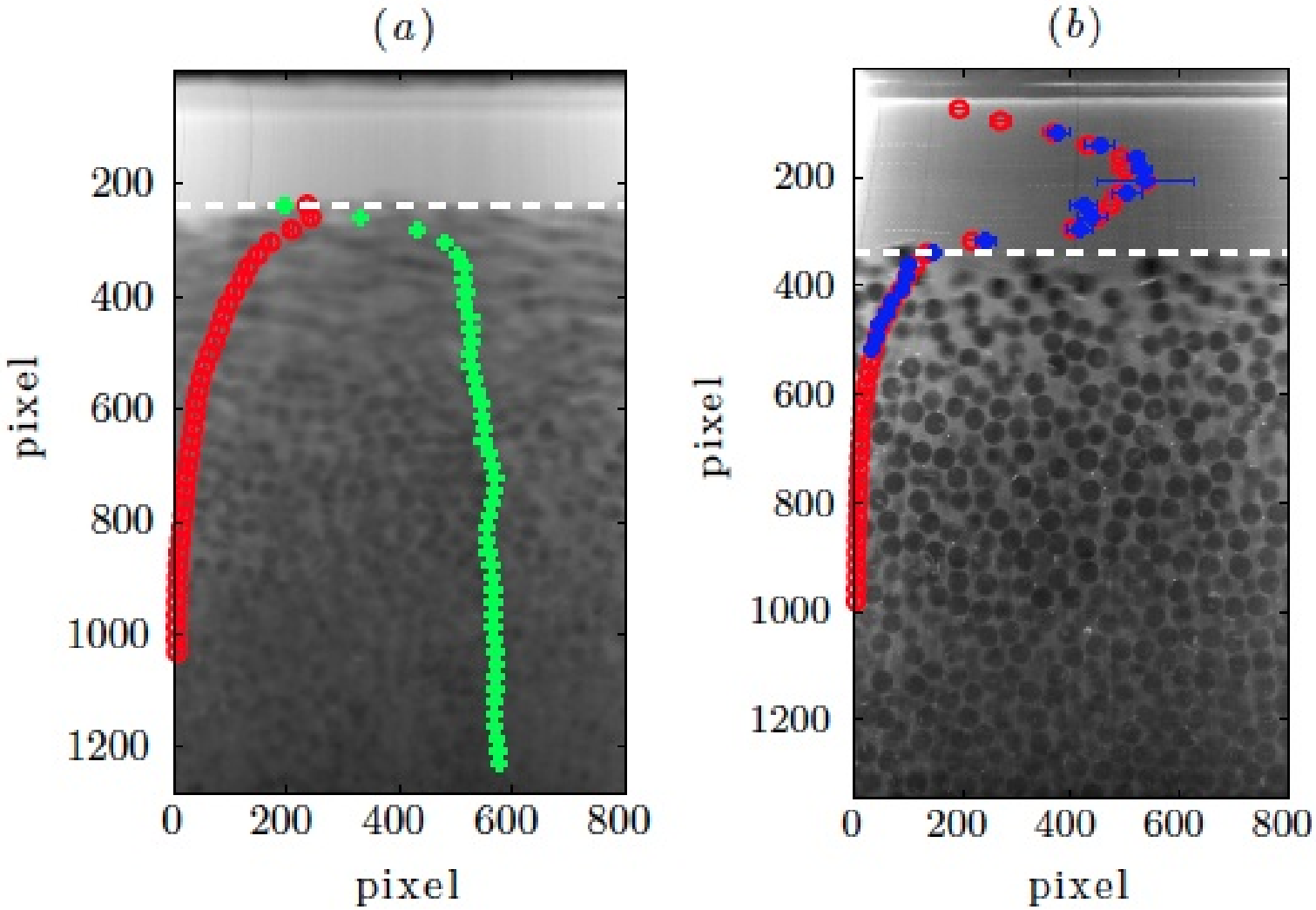

Green = Volume fraction (100 pix = 0.1)

Red = Particles velocity (110 pix = 2.5mm/s)

Blue = Fluid Velocity

No velocity slip between fluid and particles

PIV : DPIVsoft (Meunier & Leweke 2003)

Particle velocity flux and flowing layer thickness

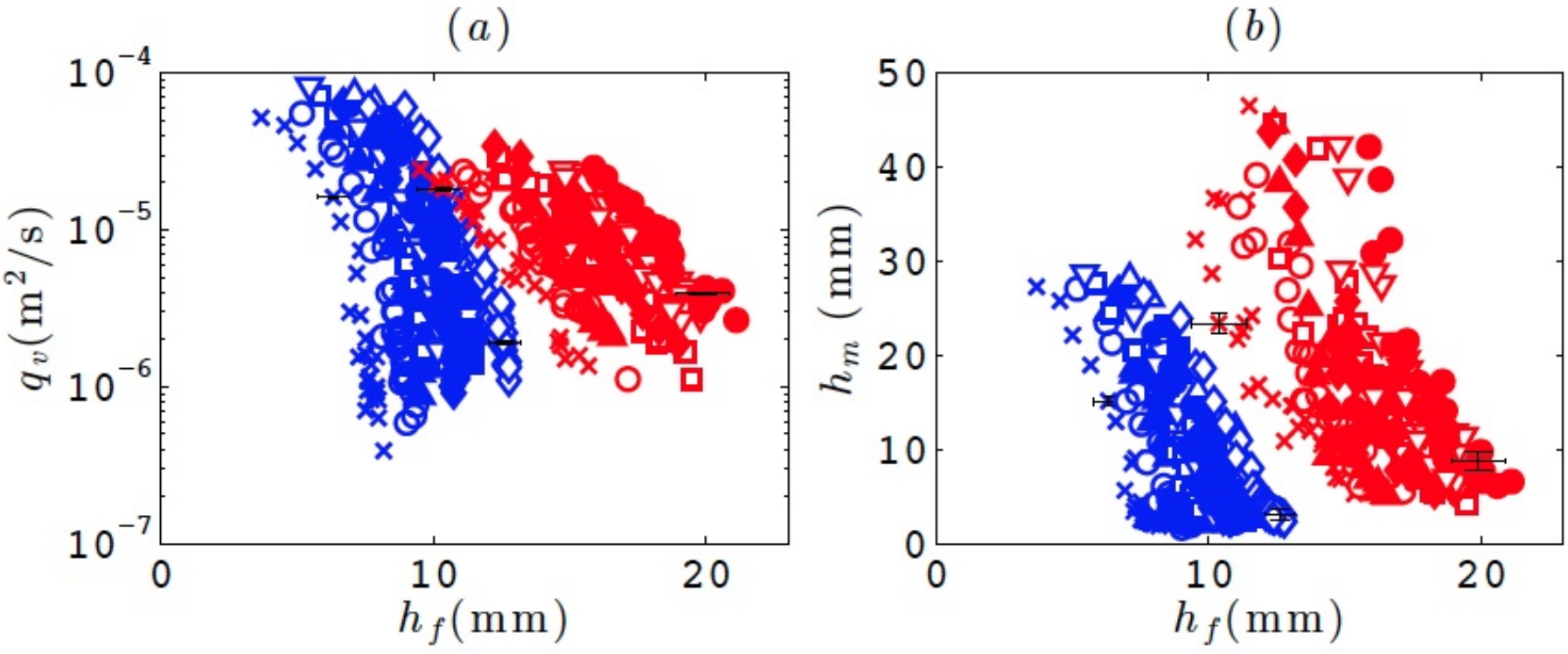

300 velocity profiles $\Rightarrow$ 300 points

$q_v = \int_{h_c}^{h_p} u_s dz$: particle velocity flux $\Rightarrow$ Less uncertainty than particle flux

$h_m = h_p - h_c$ where h_c is defined from a velocity threshold (0.09 mm/s)

Red = Borosilicate 1mm and Blue = PMMA 2mm

Two-phase model for laminar bed-load regime

$$\begin{cases} \epsilon, \phi & : \text{Volume fractions} \\ \overrightarrow{u^f}, \overrightarrow{u^p} & : \text{Average velocities} \\ \overline{\overline{\sigma^f}}, \overline{\overline{\sigma^p}} & : \text{Stress tensors} \\ n\overrightarrow{f} & : \text{Force fluid} \leftrightarrow \text{particle} \end{cases}$$

- **Continuity equations**

$$\frac{\partial \epsilon}{\partial t} + \overrightarrow{\nabla}.\left(\epsilon \overrightarrow{u^f}\right) = 0 \qquad \frac{\partial \phi}{\partial t} + \overrightarrow{\nabla}.\left(\phi \overrightarrow{u^p}\right) = 0 \qquad \epsilon + \phi = 1$$

- **Momentum equations**

$$\rho_f \left[\frac{\partial \epsilon \overrightarrow{u^f}}{\partial t} + \overrightarrow{\nabla}.\left(\epsilon \overrightarrow{u^f} \otimes \overrightarrow{u^f}\right)\right] = -p^f \overline{\overline{I}} + \overrightarrow{\nabla}.\left(\overline{\overline{\tau^f}}\right) - n\overrightarrow{f} + \epsilon \rho_f \overrightarrow{g}$$

$$\underbrace{\rho_p \left[\frac{\partial \phi \overrightarrow{u^p}}{\partial t} + \overrightarrow{\nabla}.\left(\phi \overrightarrow{u^p} \otimes \overrightarrow{u^p}\right)\right]}_{Inertia} = \underbrace{-p^p \overline{\overline{I}} + \overrightarrow{\nabla}.\left(\overline{\overline{\tau^p}}\right)}_{Stresses} + \underbrace{n\overrightarrow{f}}_{Interaction} + \underbrace{\phi \rho_p \overrightarrow{g}}_{Gravity}$$

Closures

- **Newtonian rheology** for the fluid phase → Einstein correction (bed layer)
- **Granular rheology** for the particle phase → **Friction**: $\mu(I_v)$ or Coulomb
- **Particle-fluid interaction** → Darcy + Buoyancy

Ouriemi, Aussillous & Guazzelli J. Fluid Mech. 2009 (Part 1)

A simple calculation

Mixture momentum balance at steady state

$$\tau^m(z) = \tau^p(z) + \tau^f(z) = \tau^f(h_p) - \frac{\partial p^f}{\partial x}(h_p - z)$$

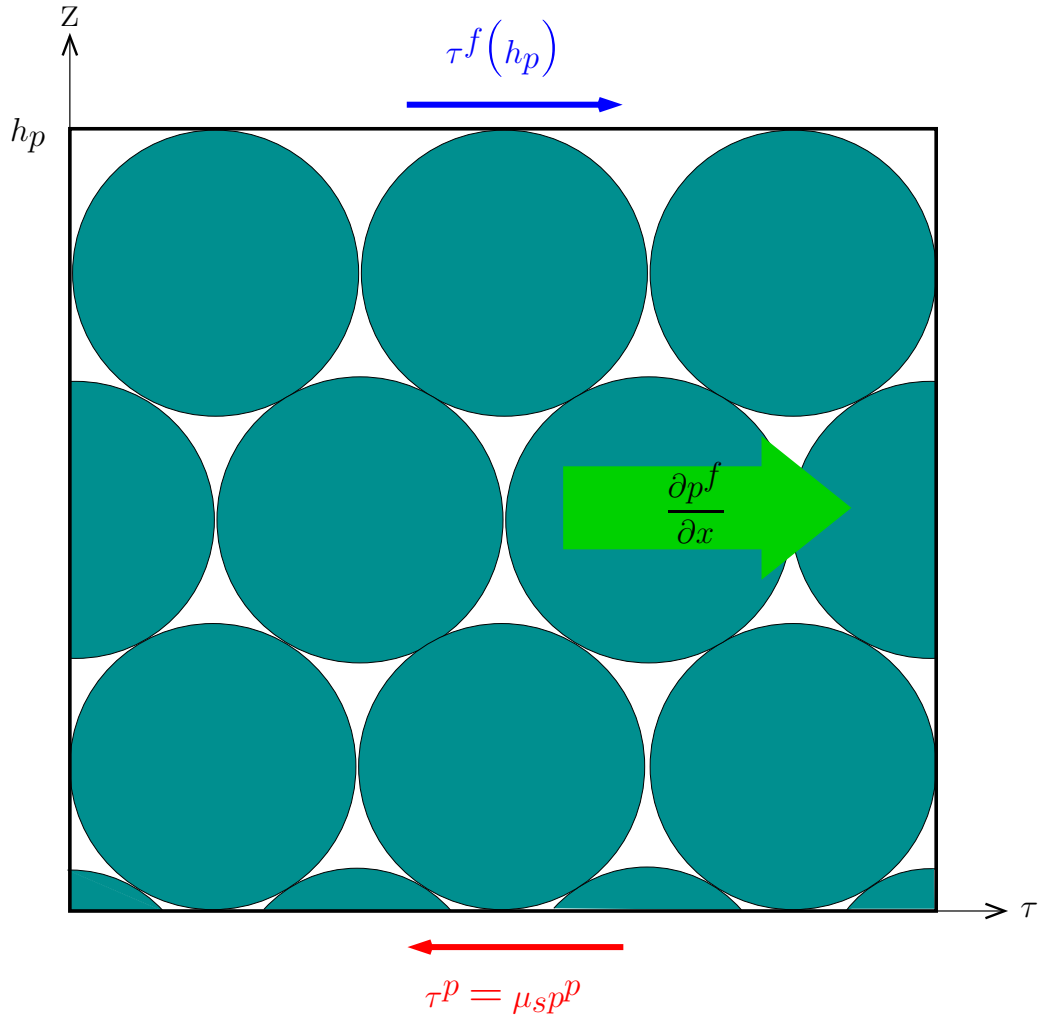

A simple calculation

Mixture momentum balance at steady state

$$\tau^m(z) = \tau^p(z) + \tau^f(z) = \tau^f(h_p) - \frac{\partial p^f}{\partial x}(h_p - z)$$

Hydrostatic particle pressure:

$p^p = \phi_0 \Delta\rho g(h_p - z)$

Particle shear stress: Coulomb

$\tau^p \leq \mu_s p^p = \mu_s \phi_0 \Delta\rho g(h_p - z)$

Fluid shear stress:

$\tau^f = \eta_e \dfrac{\partial u^f}{\partial z}$

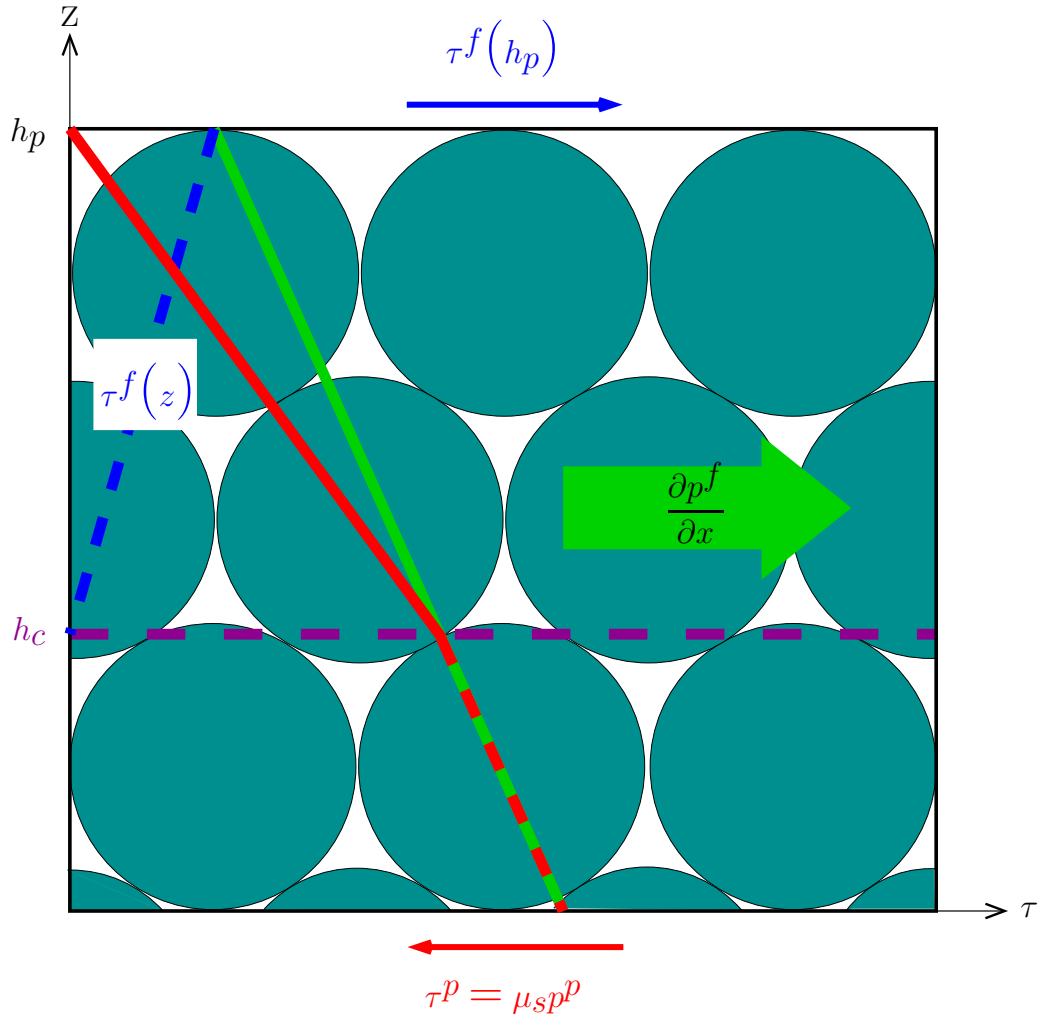

A simple calculation

Mixture momentum balance at steady state

$$\tau^m(z) = \tau^p(z) + \tau^f(z) = \tau^f(h_p) - \frac{\partial p^f}{\partial x}(h_p - z)$$

Hydrostatic particle pressure:

$$p^p = \phi_0 \Delta\rho g (h_p - z)$$

Particle shear stress: Coulomb

$$\tau^p \leq \mu_s p^p = \mu_s \phi_0 \Delta\rho g (h_p - z)$$

Fluid shear stress:

$$\tau^f = \eta_e \frac{\partial u^f}{\partial z}$$

Mixture velocity profile:

$$u^p \approx u^f = \frac{(\mu\phi_0\Delta\rho g + \frac{\partial p^f}{\partial x})}{\eta_e} \frac{(z-h_c)^2}{2}$$

Particle flux:

$$q^p = \frac{\Delta\rho g h_f^3}{\eta_f} \left[\frac{\phi_0}{6} \frac{\eta_f}{\eta_e} \left(\frac{h_m}{h_f} \right)^3 \left(\frac{\partial p^f / \partial x}{\Delta\rho g} + \mu_s \phi_0 \right) \right]$$

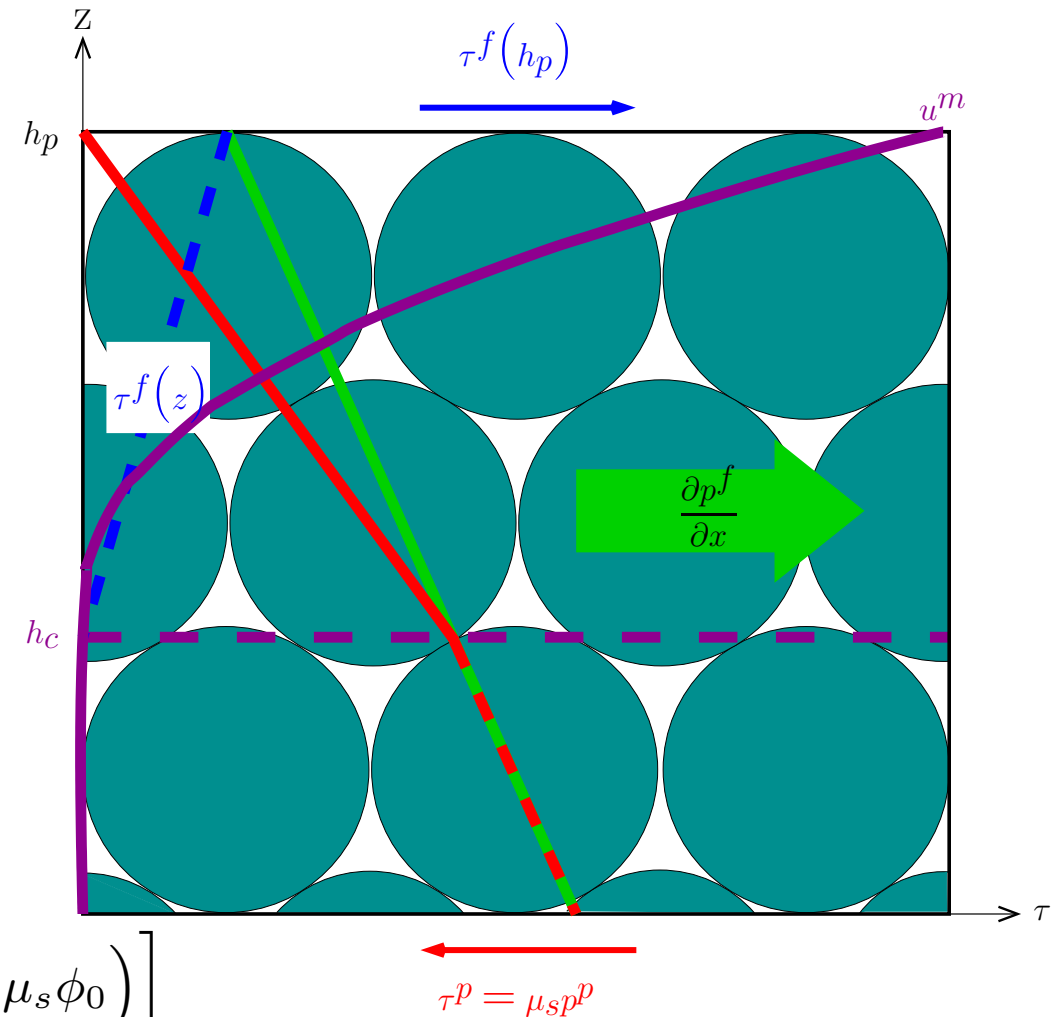

(Ouriemi et al., 2009)

Three rheological laws tested

(i) Coulomb model: (Ouriemi *et al.*,2009)

- Constant friction coefficient: $\mu = \mu_s$
- Einstein viscosity: $\eta_e = \eta_f(1 + 2.5\ \phi_0) \approx 2.4\eta_f$
- Constant volume fraction: $\phi = 0.55$

(ii) Dense granular rheology:

- Shear-rate-dependent friction coefficient $\mu(I_v)$ (e.g. Forterre & Pouliquen 2008)
- Effective viscosity: $\eta_e = \eta_f \beta$
- Constant volume fraction: $\phi = 0.55$

(iii) Dense granular rheology+variable volume fraction

- Shear-rate-dependent friction coefficient $\mu(I_v)$
- Effective viscosity: $\dfrac{\eta_e}{\eta_f} = 1 + \dfrac{5}{2}\phi\left(1 - \dfrac{\phi}{\phi_{max}}\right)^{-1}$
- Volume fraction: $\phi(I_v) = \dfrac{\phi_{max}}{1 + I^{1/2}}$

  both are deduced from pressure-imposed rheological measurements of dense suspensions of neutrally-buoyant spheres (Boyer *et al.*, 2011)

Finite Element Model

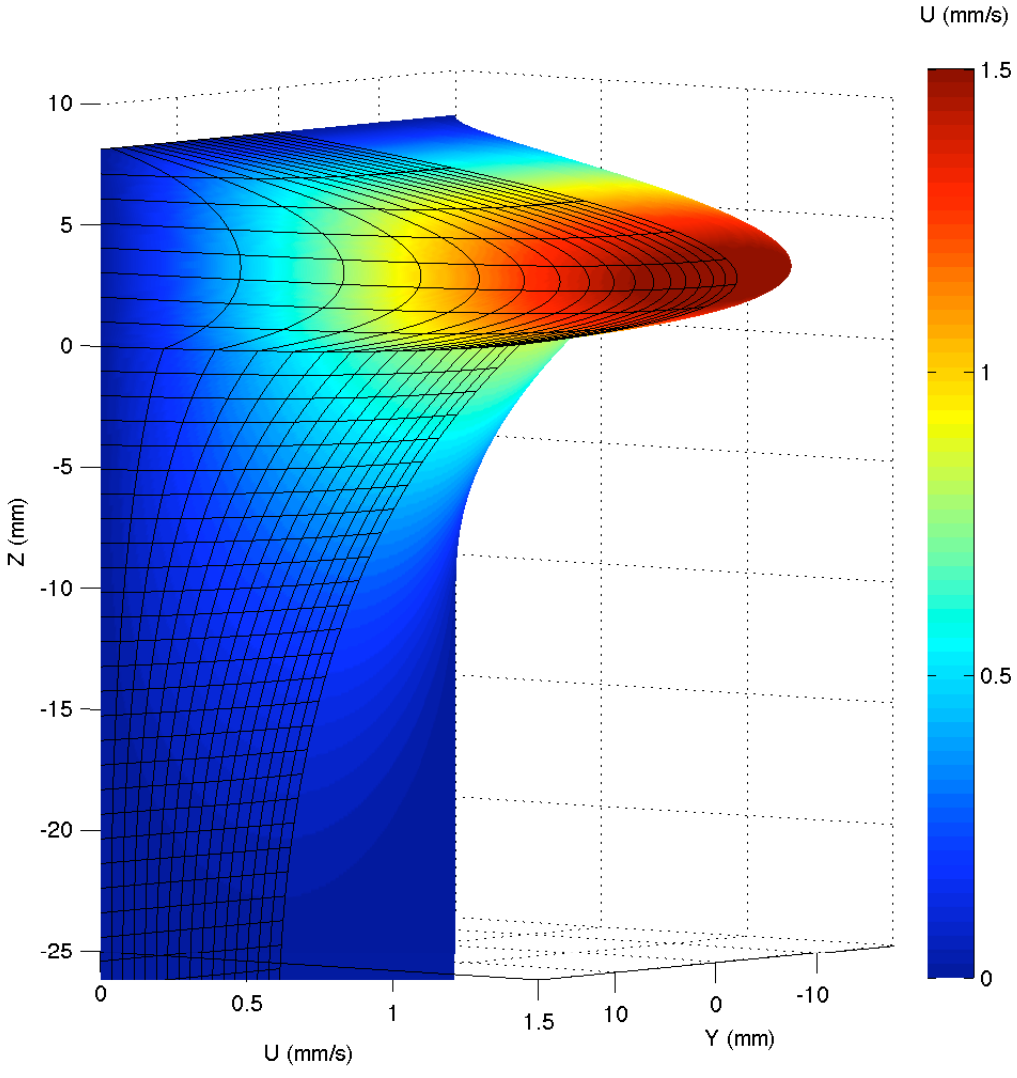

Numerical model (M. Médale)

- 3D Navier-Stokes equations
- Finite Element Method
  - Velocity: Quadratic elements
  - Pressure: Linear elements
- Newton-Raphson algorithm

Rheology implementation and BC's

- Regularisation technique for the frictional rheology
- No-slip boundary conditions at the walls

Chauchat & Médale (2010, 2013)

Scaling laws

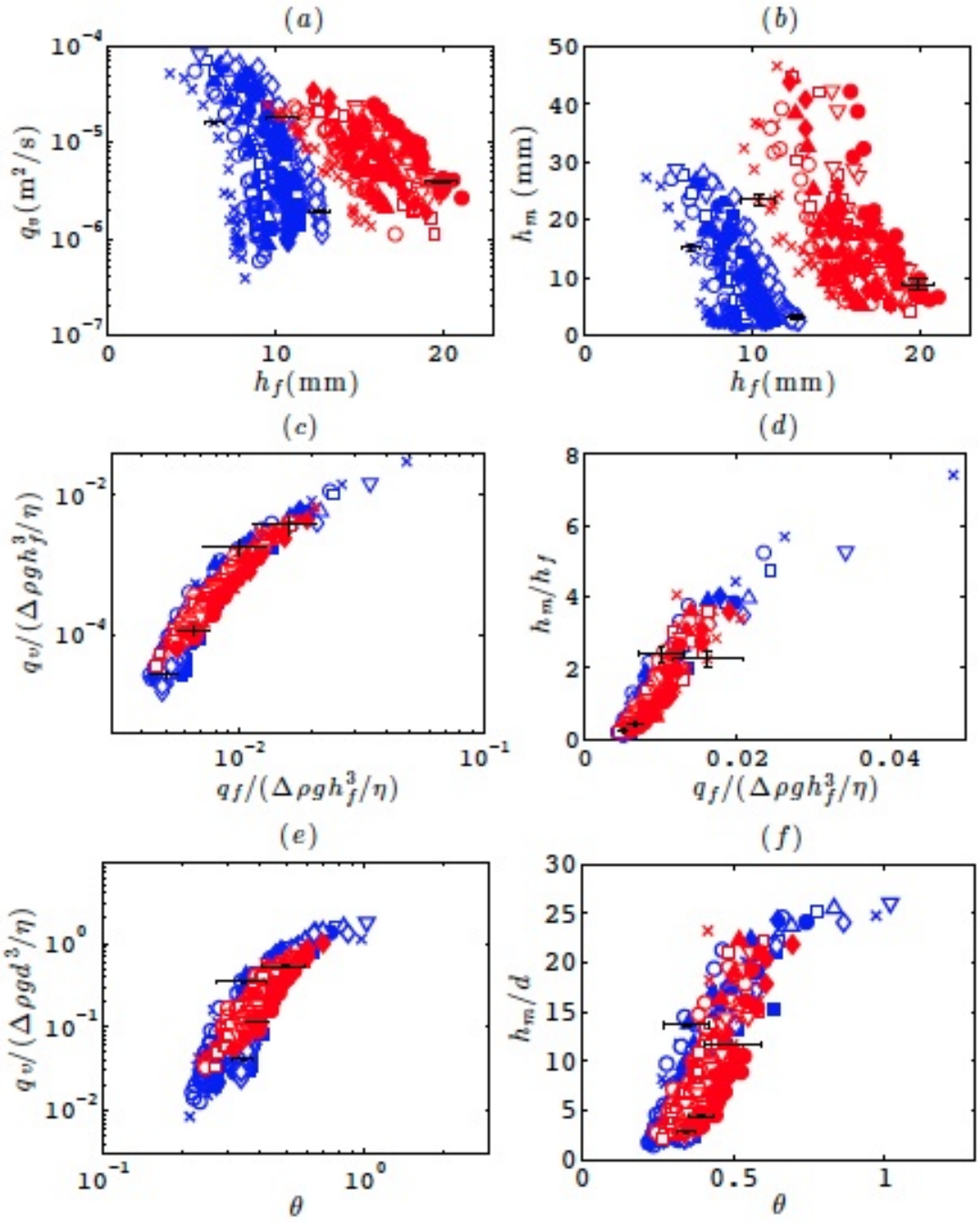

Two-phase model scaling:

$L = h_f$ and $T = \dfrac{\eta}{\Delta\rho g h_f}$

$\Rightarrow \dfrac{q_f}{\Delta\rho g h_f^3/\eta}$ good control parameter

Classic bed-load scaling:

control parameter: Shields number θ

Scaling laws

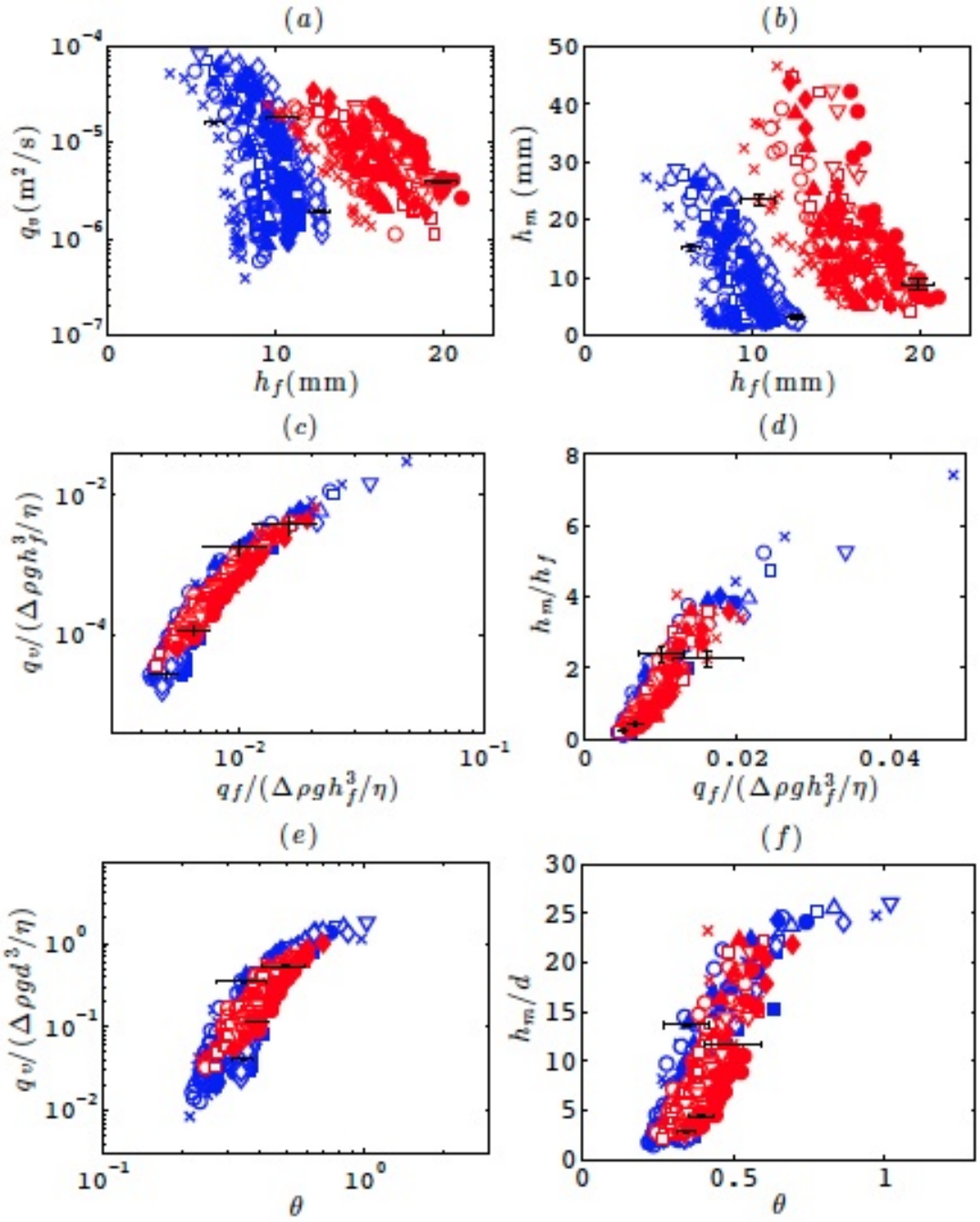

Better collapse of the data with the two-phase scaling

But still the Shields scaling can be seen as appropriate

Two-phase model scaling:

$L = h_f$ and $T = \dfrac{\eta}{\Delta\rho g h_f}$

$\Rightarrow \dfrac{q_f}{\Delta\rho g h_f^3/\eta}$ good control parameter

Classic bed-load scaling:

control parameter: Shields number θ

Data model comparison: Particle flux and flowing layer thickness

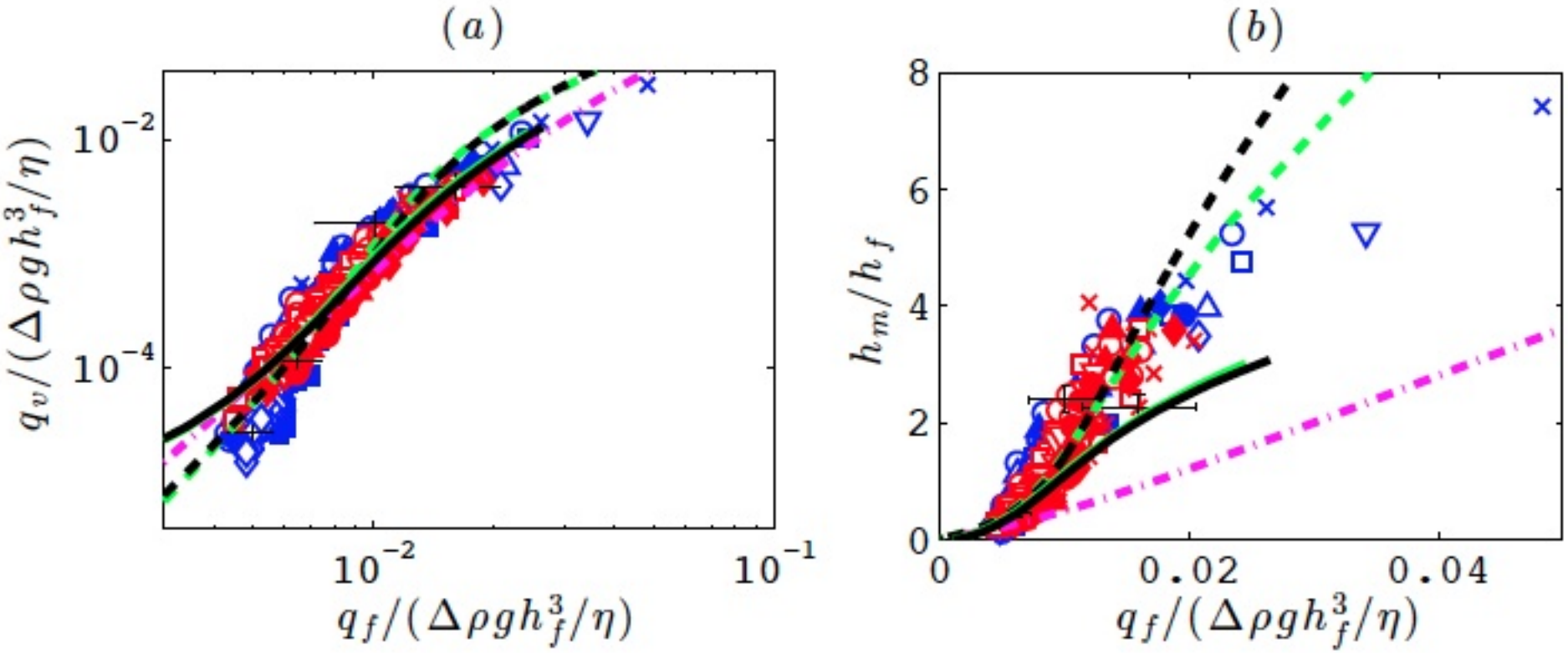

–·– Coulomb 2D: $\mu_s = 0.32$ and $\eta_e/\eta = 2.4$ (Einstein with $\phi = 0.55$)

Data model comparison: Particle flux and flowing layer thickness

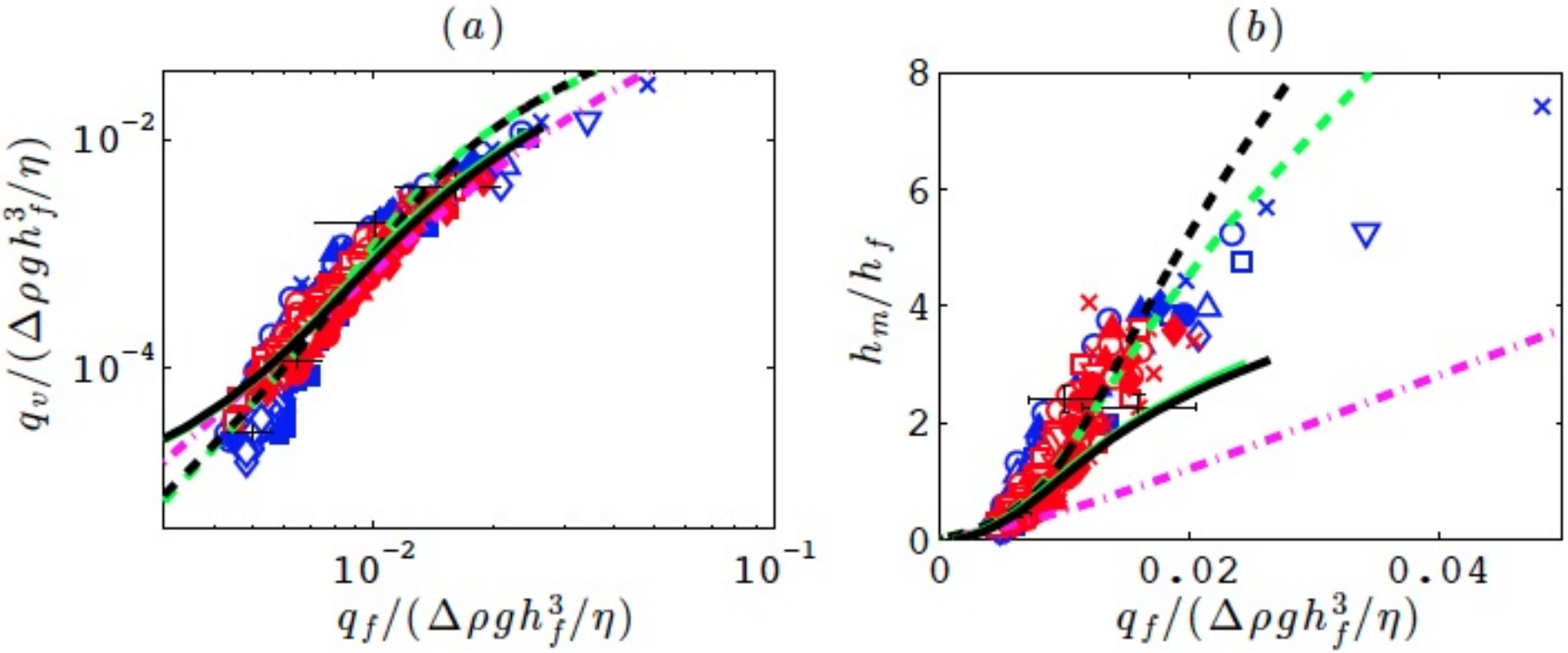

–·– Coulomb 2D: $\mu_s = 0.32$ and $\eta_e/\eta = 2.4$ (Einstein with $\phi = 0.55$)

$\Rightarrow$ Best fit of the rheological parameter

Data model comparison: Particle flux and flowing layer thickness

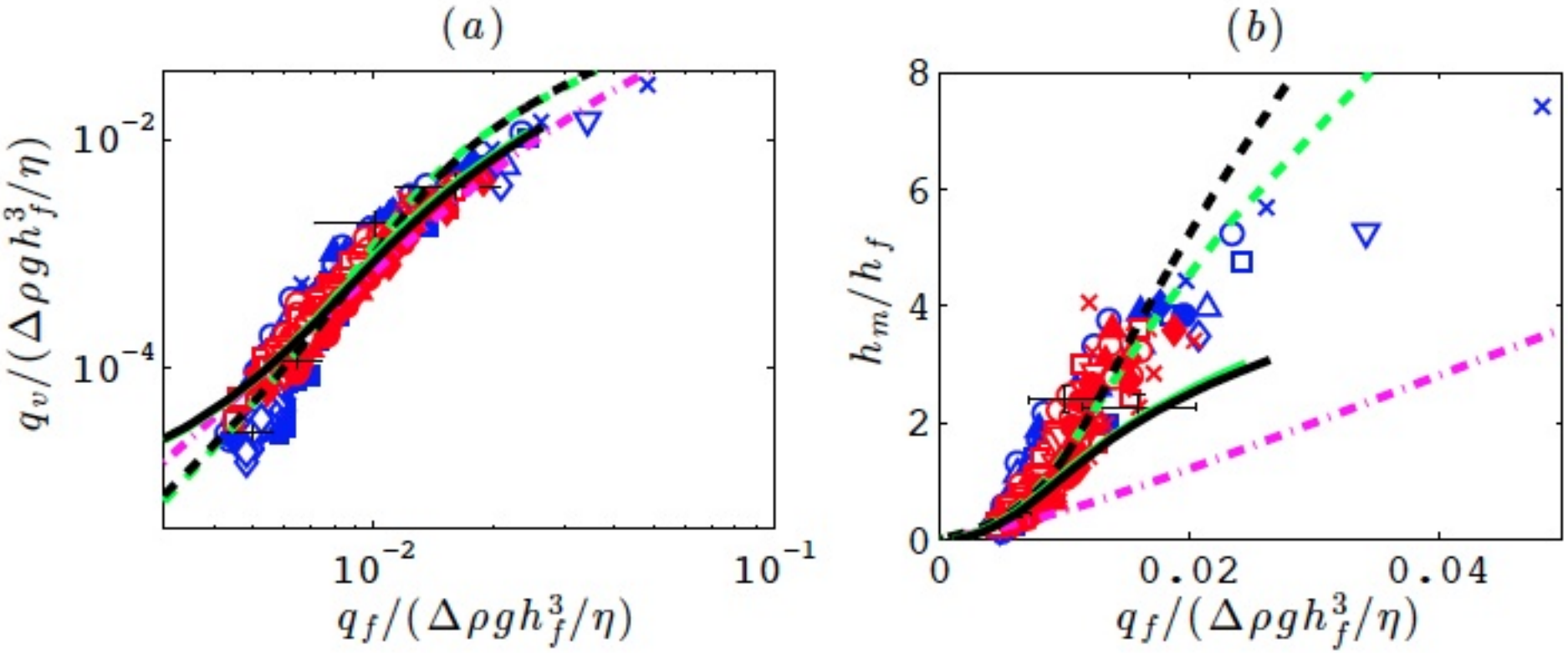

–·– Coulomb 2D: $\mu_s = 0.32$ and $\eta_e/\eta = 2.4$ (Einstein with $\phi = 0.55$)

$\Rightarrow$ Best fit of the rheological parameter

– – Coulomb 2D: $\mu_s = 0.24$ and $\eta_e/\eta = 14$ (least square fit)

Data model comparison: Particle flux and flowing layer thickness

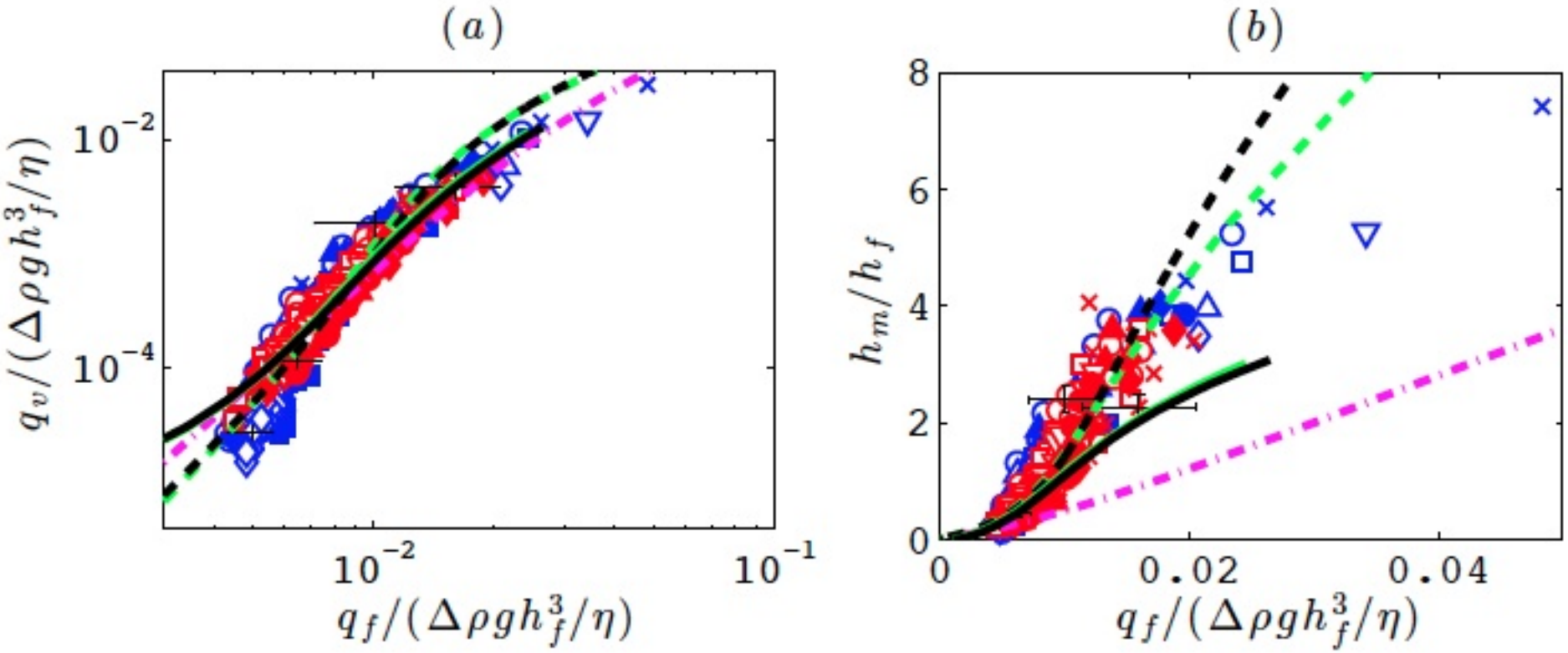

–·– Coulomb 2D: $\mu_s = 0.32$ and $\eta_e/\eta = 2.4$ (Einstein with $\phi = 0.55$)

$\Rightarrow$ Best fit of the rheological parameter

– – Coulomb 2D: $\mu_s = 0.24$ and $\eta_e/\eta = 14$ (least square fit)

—— Coulomb 3D: $\mu_s = 0.24$ and $\eta_e/\eta = 14$ $\Rightarrow$ 3D effects arise for $\overline{q_f} \geq 10^{-2}$

Data model comparison: Particle flux and flowing layer thickness

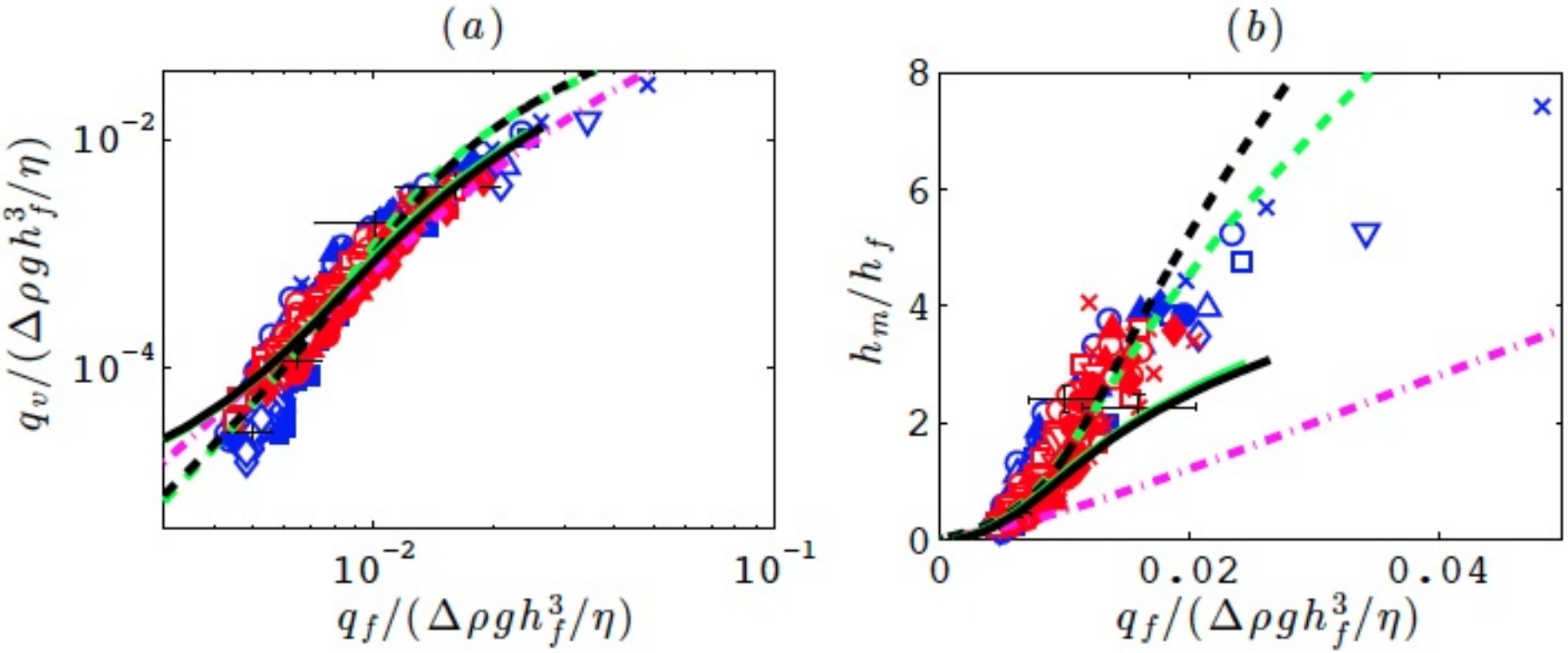

–·– Coulomb 2D: $\mu_s = 0.32$ and $\eta_e/\eta = 2.4$ (Einstein with $\phi = 0.55$)

$\Rightarrow$ Best fit of the rheological parameter

– – Coulomb 2D: $\mu_s = 0.24$ and $\eta_e/\eta = 14$ (least square fit)

—— Coulomb 3D: $\mu_s = 0.24$ and $\eta_e/\eta = 14$ $\Rightarrow$ 3D effects arise for $\overline{q_f} \geq 10^{-2}$

– – $\mu(I)$ 2D: $\mu_s = 0.24$, $\mu_2 = 0.39$, $I_0 = 0.01$ and $\eta_e/\eta = 6.6$ (least square fit)

Data model comparison: Particle flux and flowing layer thickness

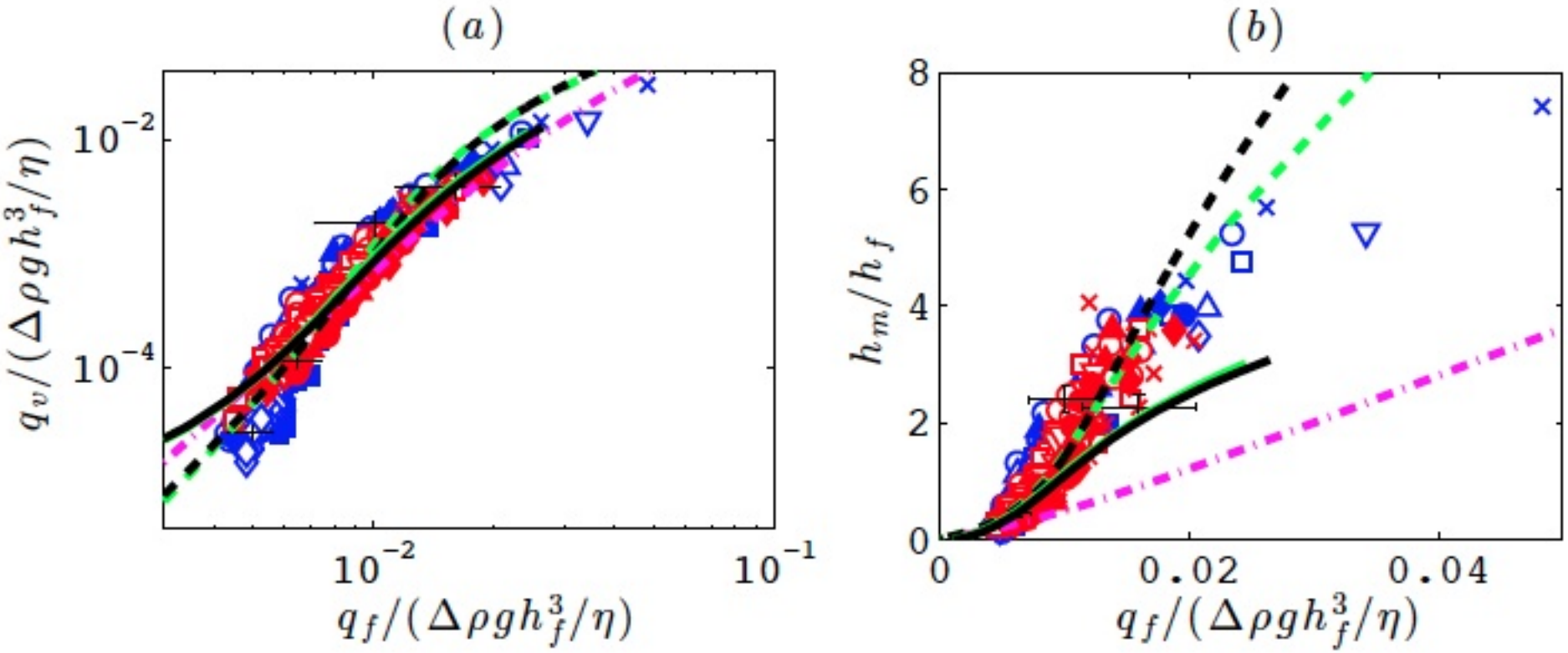

–·– Coulomb 2D: $\mu_s = 0.32$ and $\eta_e/\eta = 2.4$ (Einstein with $\phi = 0.55$)

⇒ Best fit of the rheological parameter

– – Coulomb 2D: $\mu_s = 0.24$ and $\eta_e/\eta = 14$ (least square fit)

—— Coulomb 3D: $\mu_s = 0.24$ and $\eta_e/\eta = 14$ ⇒ 3D effects arise for $\overline{q_f} \geq 10^{-2}$

– – $\mu(I)$ 2D: $\mu_s = 0.24$, $\mu_2 = 0.39$, $I_0 = 0.01$ and $\eta_e/\eta = 6.6$ (least square fit)

—— $\mu(I)$ 3D: $\mu_s = 0.24$, $\mu_2 = 0.39$, $I_0 = 0.01$ and $\eta_e/\eta = 6.6$

Data model comparison: Velocity profiles

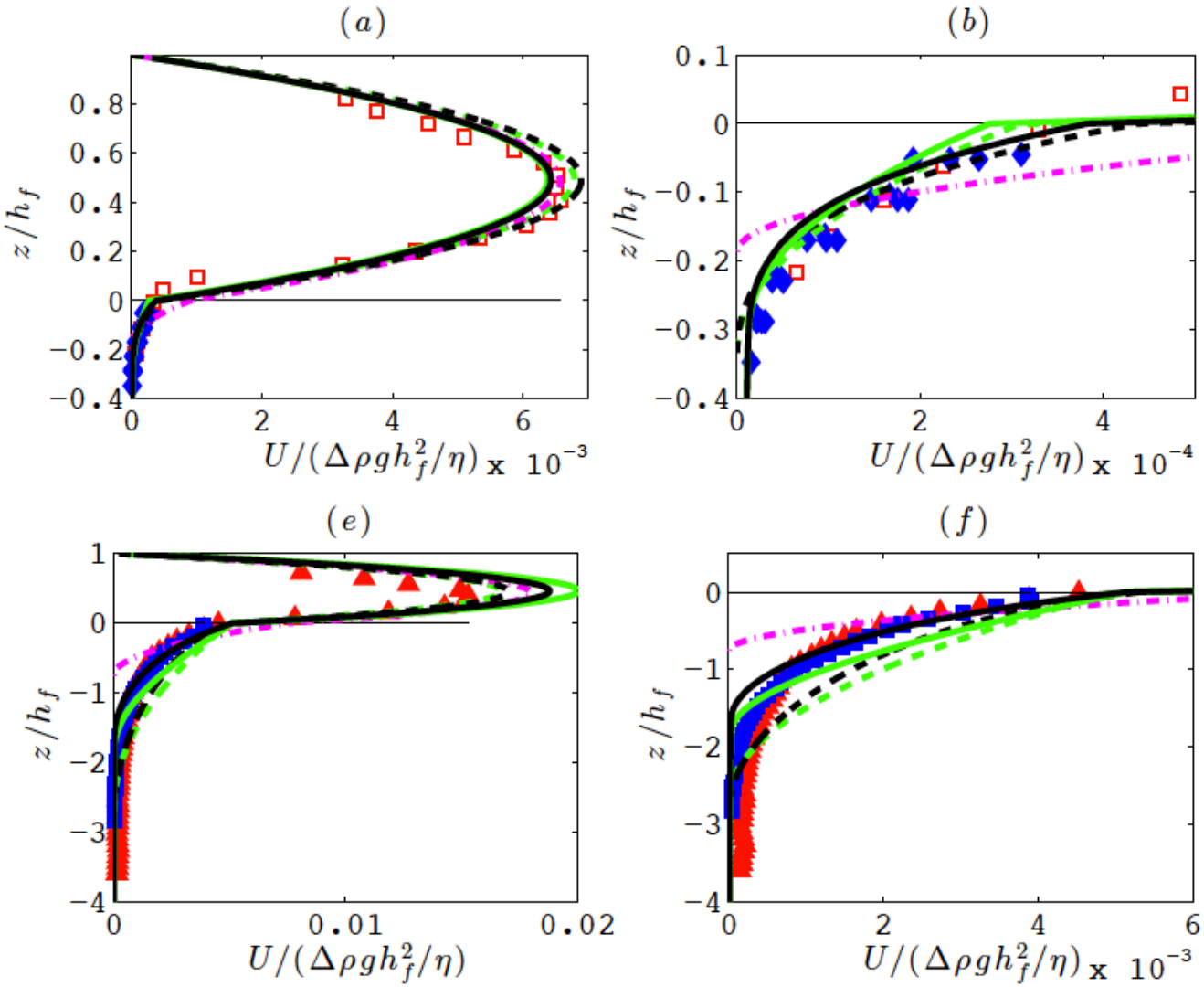

- Coulomb 2D: $\mu_s = 0.32\,;\ \eta_e/\eta = 2.4$
- Coulomb 2D: $\mu_s = 0.24\,;\ \eta_e/\eta = 14$
- Coulomb 3D: $\mu_s = 0.24\,;\ \eta_e/\eta = 14$
- $\mu(I)$ 2D: $\mu_s = 0.24$, $\mu_2 = 0.39$, $I_0 = 0.01$ and $\eta_e/\eta = 6.6$
- $\mu(I)$ 3D: $\mu_s = 0.24$, $\mu_2 = 0.39$, $I_0 = 0.01$ and $\eta_e/\eta = 6.6$

- Coulomb 2D $\mu_s = 0.32\,;\ \eta_e/\eta = 2.4$
  $\rightarrow$ h_m underestimated and $U(z)$ overstimated $\Rightarrow$ compensation on q_v
- Fitted Coulomb and $\mu(I)$ rheologies $\Rightarrow$ Clear 3D effects for both
  $\rightarrow$ More refined $\mu(I)$ rheology has a much reasonable effective viscosity

Data model comparison: Dense granular rheology+variable volume fraction

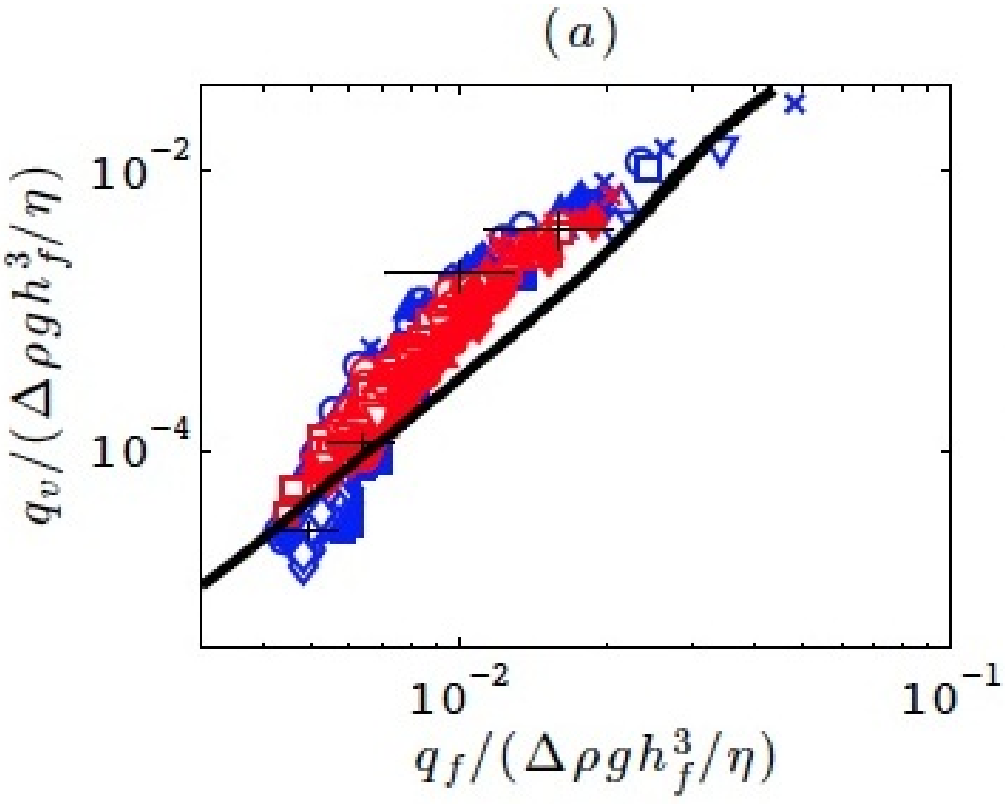

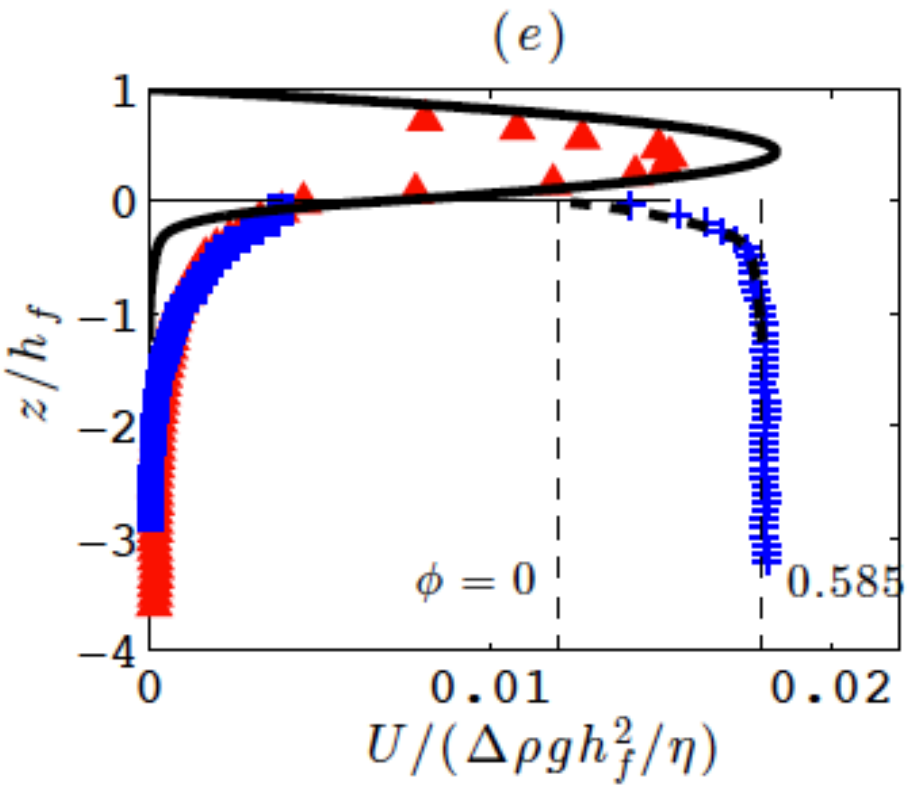

Good order of magnitude but too stiff velocity profiles however ϕ is good ($\phi \approx cst$)

$\rightarrow$ Non-buoyant rheology $\neq$ Buoyant rheology

$\rightarrow$ Validity of a continuum approach at the fluid-bed interface

$\rightarrow$ Pore pressure effects

Conclusions: laminar bed-load

Experiments

- No significant slip between fluid and particles
- Volume fraction approximately constant (except at the bed interface)
- Scaling: fluid height as length scale / Viscous timescale
  $\rightarrow$ Shields OK but not that good

Models

- Coulomb $\rightarrow$ good prediction for q_v but not for h_m and $U(z)$
- Fitted rheological parameters $\rightarrow$ good predictions and 3D effects recovered
  $\rightarrow$ $\mu(I)$ corresponds to more realistic effective viscosity
- Boyer *et al.* (2011) rheological model ($\mu(I)$ and $\phi(I)$)
  $\rightarrow$ Good trend and order of magnitude but fails in predicting velocity profiles

$\Rightarrow$ Why original parameters do not fit: non-equilibrium experiments? rheology is different for neutrally-buoyant and buoyant particles? Modelling a sharp interface as continuum?

$\Rightarrow$ **Two-Phase continuum model having a frictional rheology is able to describe intense bed-load transport in laminar shearing flows.**

Accepted for publication in JFM: Aussillous, Chauchat, Pailha, Médale and Guazzelli

1. Introduction

2. Laminar bed-load
   - Experiments:Index-matching technique
   - Modeling approaches:Two-phase model
   - Model data comparisons

3. Sheet-flow of massive particles
   - Modeling approach
   - Validation and comparison with literature data
   - Sheet-flow experiments at LEGI

4. Conclusions and on-going work

This work has been done in collaboration with **Thibaud Revil-Baudard**, David Hurther, Hervé Michallet and Eric Barthélémy at the LEGI Lab in Grenoble (France) and Patrick Snabre from the CRPP at the University of Bordeaux.

1. Introduction

2. Laminar bed-load
   - Experiments:Index-matching technique
   - Modeling approaches:Two-phase model
   - Model data comparisons

3. Sheet-flow of massive particles
   - Modeling approach
   - Validation and comparison with literature data
   - Sheet-flow experiments at LEGI

4. Conclusions and on-going work

Two-phase model for turbulent sheet-flow regime

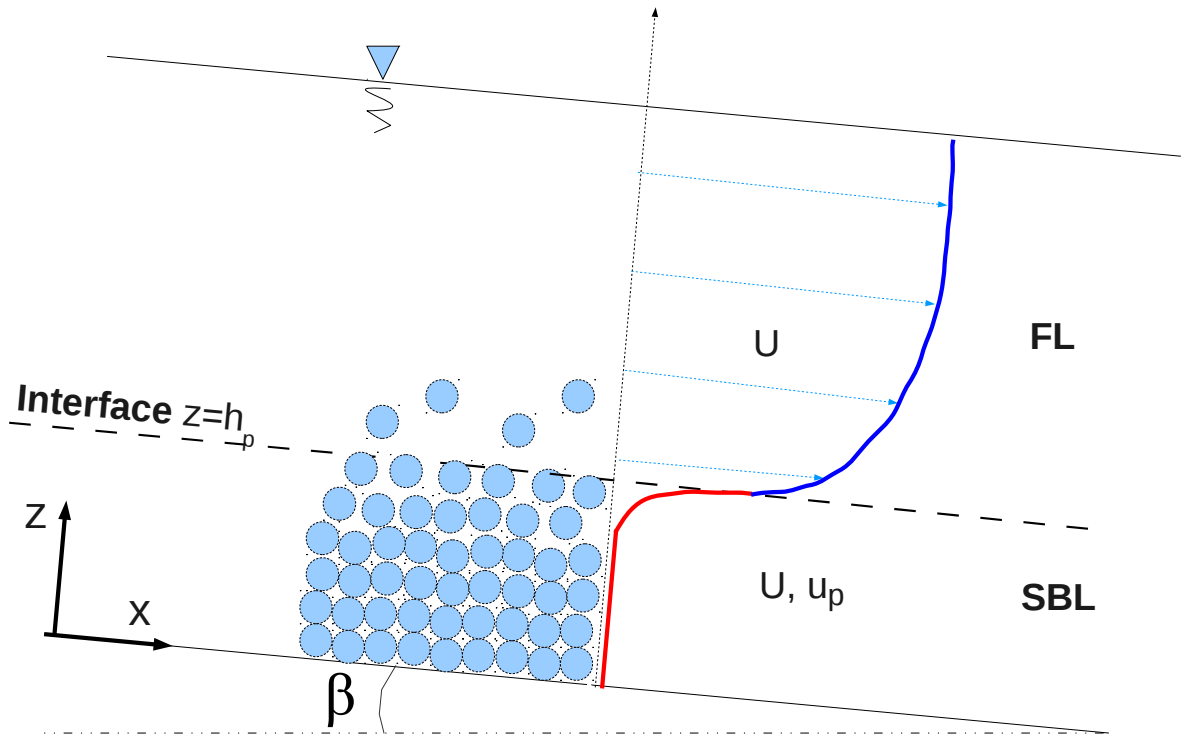

Two layers:

- Fluid Layer (FL)
  $\longrightarrow$ single fluid model
  $\longrightarrow$ passive scalar
- Sediment Bed Layer (SBL)
  $\longrightarrow$ two-phase model

- Unidirectional: $u^f = u^f(z)$ and $u^p = u^p(z)$
- Uniform: $\dfrac{\partial}{\partial x} = 0$
- Steady: $\dfrac{\partial}{\partial t} = 0$ and $w^f = w^p = 0$

Revil-Baudard and Chauchat JGR (2013)

Two-phase model in the SBL

$$\begin{cases} \epsilon, \phi & : \text{Volume fractions} \\ \overrightarrow{u^f}, \overrightarrow{u^p} & : \text{Average velocities} \\ n\overrightarrow{f} & : \text{Force fluid} \leftrightarrow \text{particle} \end{cases}$$

- **Continuity equations**

$$\frac{\partial \epsilon}{\partial t} + \overrightarrow{\nabla}.\left(\epsilon \overrightarrow{u^f}\right) = 0 \qquad \frac{\partial \phi}{\partial t} + \overrightarrow{\nabla}.\left(\phi \overrightarrow{u^p}\right) = 0 \qquad \epsilon + \phi = 1$$

- **Momentum equations**

$$\rho_f \left[\frac{\partial \epsilon \overrightarrow{u^f}}{\partial t} + \overrightarrow{\nabla}.\left(\epsilon \overrightarrow{u^f} \otimes \overrightarrow{u^f}\right)\right] = -\overrightarrow{\nabla} p^f + \overrightarrow{\nabla}.\left(\overline{\overline{\tau^f}} + \overline{\overline{R^f}}\right) - n\overrightarrow{f} + \epsilon \rho_f \overrightarrow{g}$$

$$\underbrace{\rho_p \left[\frac{\partial \phi \overrightarrow{u^p}}{\partial t} + \overrightarrow{\nabla}.\left(\phi \overrightarrow{u^p} \otimes \overrightarrow{u^p}\right)\right]}_{Inertia} = \underbrace{-\overrightarrow{\nabla} p^p + \overrightarrow{\nabla}.\left(\overline{\overline{\tau^p}}\right)}_{Stresses} + \underbrace{n\overrightarrow{f}}_{Interaction} + \underbrace{\phi \rho_p \overrightarrow{g}}_{Gravity}$$

- **Newtonian rheology** for the fluid phase ($\overline{\overline{\tau^f}}$) $\rightarrow$ Boyer *et al.* (2011)
- **Mixing length** for the Reynolds stresses ($\overline{\overline{R^f}}$) $\rightarrow$ Li and Sawamoto (1995)
- **Granular rheology** for the particle phase ($\overline{\overline{\tau^p}}$) $\rightarrow$ **Friction**: $\mu(I)$
- **Particle-fluid interaction** ($\overrightarrow{n_f}$) $\rightarrow$ Drag (Dallavalle+R&Z) + Buoyancy
- **Concentration profile** $\rightarrow$ Dilatancy $\phi(I)$ + Rouse (turbulent dispersion)

Two-phase equations

Global volume conservation: $\epsilon + \phi = 1$

Vertical momentum equations:

$$0 = -\frac{\mathrm{d}p^f}{\mathrm{d}z} - nf_z - \epsilon\rho_f g\cos\beta \qquad 0 = -\frac{\mathrm{d}p^p}{\mathrm{d}z} + nf_z - \phi\rho_p g\cos\beta$$

Archimede buoyancy force: $nf_z = -\phi\dfrac{\mathrm{d}P^f}{\mathrm{d}z}$

Two-phase equations

Global volume conservation: $\epsilon + \phi = 1$

Vertical momentum equations:

$$0 = -\frac{\mathrm{d}p^f}{\mathrm{d}z} - nf_z - \epsilon\rho_f g\cos\beta \qquad 0 = -\frac{\mathrm{d}p^p}{\mathrm{d}z} + nf_z - \phi\rho_p g\cos\beta$$

Archimede buoyancy force: $nf_z = -\phi\dfrac{\mathrm{d}P^f}{\mathrm{d}z}$

$$\frac{\mathrm{d}p^f}{\mathrm{d}z} = -\rho_f g\cos\beta \qquad \frac{\mathrm{d}p^p}{\mathrm{d}z} = -\phi(\rho_p - \rho_f)g\cos\beta$$

$\Rightarrow$ Hydrostatic pressure distribution for both phases

Horizontal momentum equations

$$0 = \frac{\mathrm{d}R^f_{xz}}{\mathrm{d}z} + \epsilon \frac{\mathrm{d}\tau^f_{xz}}{\mathrm{d}z} - C_D\ (U - u^p) + \epsilon\ \rho_f\ g\ \sin\beta$$

$$0 = \frac{\mathrm{d}\tau^p_{xz}}{\mathrm{d}z} + \phi \frac{\mathrm{d}\tau^f_{xz}}{\mathrm{d}z} + C_D\ (U - u^p) + \phi\ \rho_p\ g\ \sin\beta$$

where C_D is given by: $C_D = \frac{\rho_f\ \phi}{d_p\ (1-\phi)^{3.1}} \left(0.3\ (U - u^p) + 18.3\ \frac{\eta_f}{\rho_f\ d_p} \right)$

Dallavalle (1943) + Richardson and Zaki (1954)

Fluid closures:

Effective viscous stresses: $\boxed{\tau^f_{xz} = \eta_e\ \frac{\mathrm{d}U}{\mathrm{d}z}}$ where $\frac{\eta_e}{\eta_f} = 1 + 2.5\phi \left(1 - \frac{\phi}{\phi_{max}} \right)^{-1}$

$\rightarrow$ Boyer *et al.*(2011) (similar to Krieger-Dougherty's effective viscosity)

Reynolds stresses: $\boxed{R^f_{xz} = \eta_t \frac{\mathrm{d}U}{\mathrm{d}z}}$ with $\eta_t = \rho_f\ (1-\phi)\ l_m^2\ \left| \frac{dU}{dz} \right|$

and $l_m = \kappa \int_0^z \frac{\phi_{max} - \phi}{\phi_{max}} \mathrm{d}z$ (Li and Sawamoto ; 1995)

$\rightarrow$ used by Dong and Zhang (1999) to model oscillatory sheet flows.

Dense granular rheology

Frictional stress: $\boxed{\tau_{xz}^p = \mu(I) p^p}$

where $\mu(I) = \mu_s + \dfrac{\mu_2 - \mu_s}{I_0/I + 1}$ and $I = \dfrac{\left| \dfrac{\mathrm{d}u^p}{\mathrm{d}z} \right| d_p}{\sqrt{p^p/\rho_p}}$

We have shown that in sheet flow regime the granular flow is in the inertial regime

$\longrightarrow$ This is consistent with Bagnold's (1956) model

see Revil-Baudard and Chauchat (2013)

Dilatancy law: $\boxed{\phi(I) = \dfrac{\phi_{max}}{1 + b\ I^{1/2}}}$

- validity range $\phi \in [0.3; \phi_{max}]$
- same relationship as in the viscous regime
- $b = 0.75$ is added as a tunable parameter to account for non-sphericity

Single-phase model in the FL

Horizontal fluid momentum equation:

$$0 = \frac{\mathrm{d}\tau_{xz}^f}{\mathrm{d}z} + \frac{\mathrm{d}R_{xz}^f}{\mathrm{d}z} + \rho_f \; g \; \sin\beta$$

Same closures for τ_{xz}^f and R_{xz}^f as in the SBL layer

Concentration profile:

Vertical equilibrium: $w_s\phi + \dfrac{\eta_t}{\rho_f}\dfrac{\mathrm{d}\phi}{\mathrm{d}z} = 0$

$$\phi(z) = \phi_{h_p} \exp\left(-\rho_f \; w_s \int_{h_p}^{z} \eta_t^{-1} \, \mathrm{d}z\right)$$

Sumer *et al.*(1996) have shown that a Rouse profile is observed above a sheet flow layer provided that the reference level is taken high enough above the mobile bed ($\phi \geq 0.25$)

Rouse profile and dilatancy law ($\phi(I)$) can cover the whole range of concentration from the static bed up to the dilute suspension.

Resolution strategy and boundary conditions

Numerical method:

- pseudo-time integration and an implicit finite difference discretisation
- FL $\rightarrow$ tridiagonal system solved using a doublesweep algorithm
- SBL $\rightarrow$ Moore-Penrose solver (Matlab®)
- Under-relaxation for the dilatancy law

Lagrangian mesh adaptation:

- SBL $\rightarrow$ mass conservation in each cell

  $\Rightarrow \Delta z$ is varied to account for bed decompation

- FL $\rightarrow$ the eroded volume of sediment is subtracted from the SBL (uniformly)

  $\Rightarrow$ The sediment volume conservation is about 99.9%

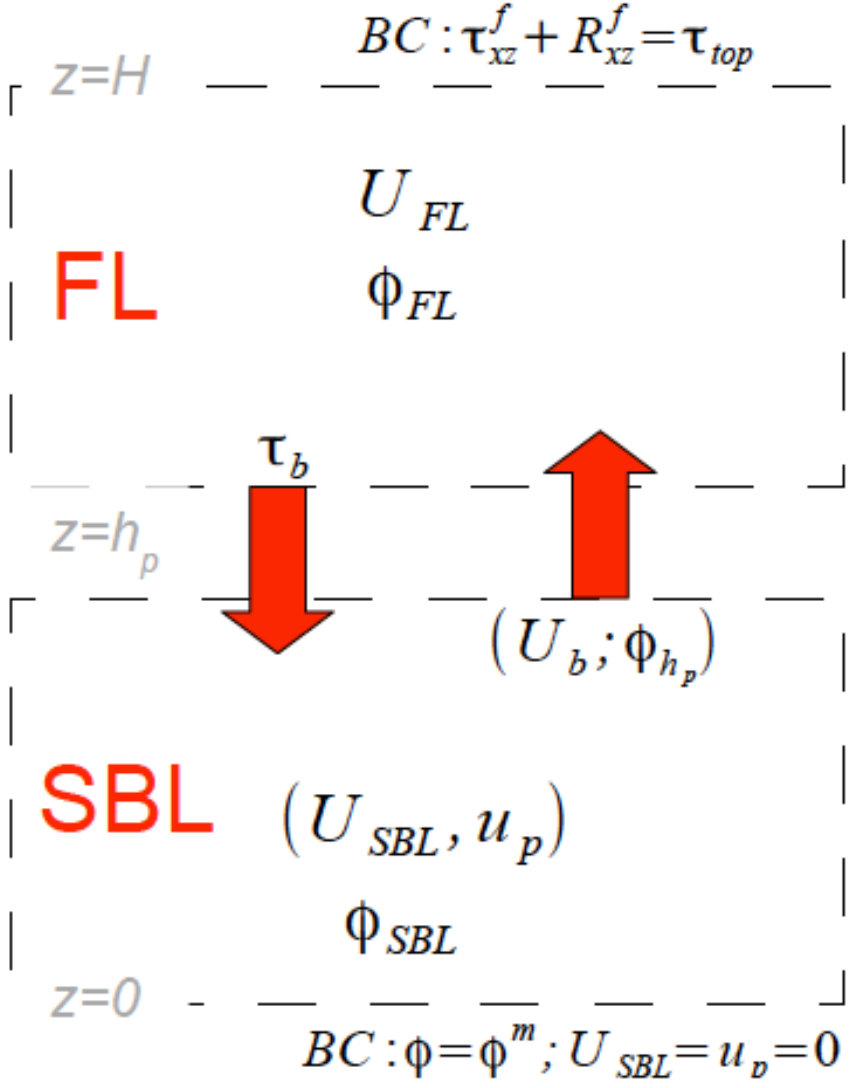

Comparison with Sumer *et al.* experiments: velocity profiles

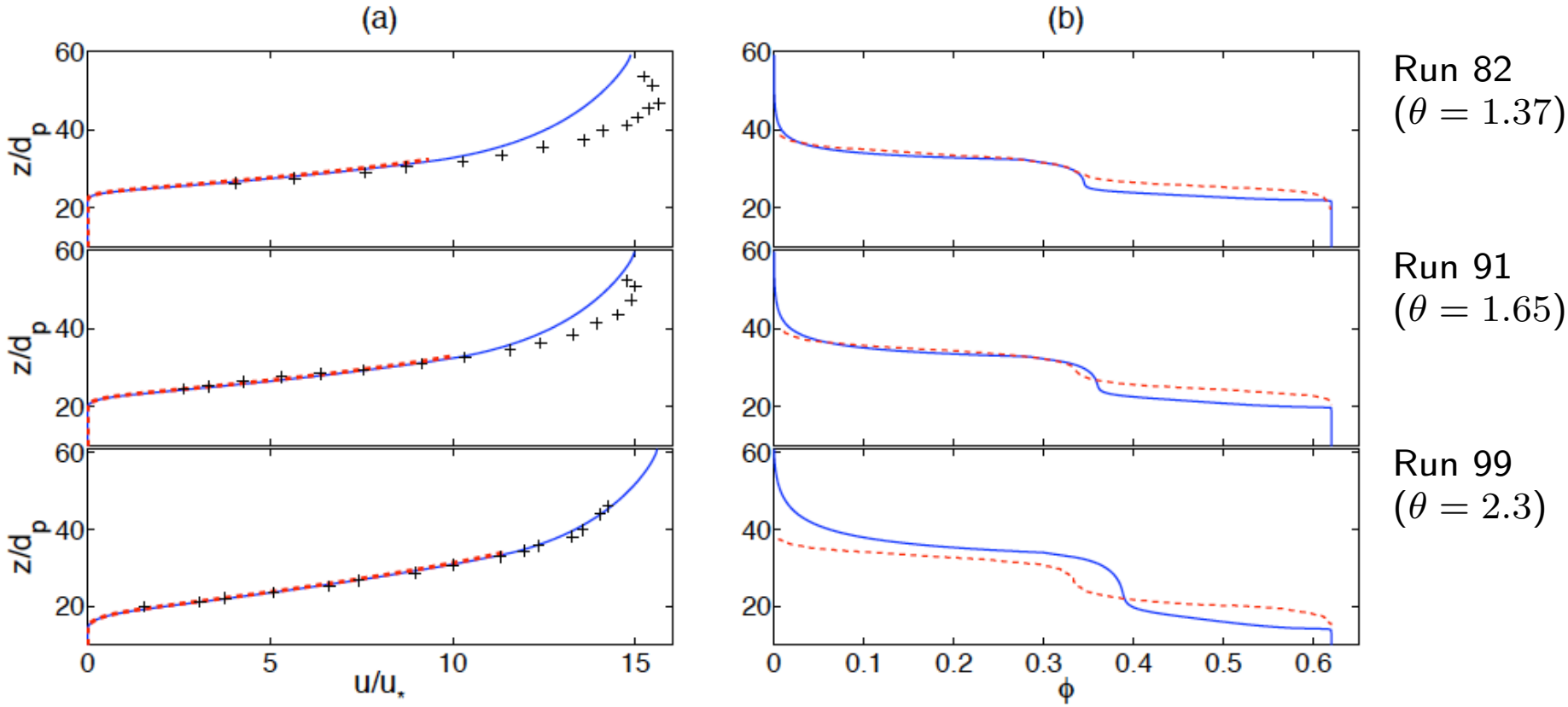

Fig. : Comparison of the fluid (—) and the particulate (- - -) velocity profiles between the present model and the measurements of Sumer *et al.* (1996) (+) in (a) and comparison of the concentration profiles predicted by the present model (—) with Hsu *et al.*'s (2004) results (- - -) in (b).

$\mu_s = 0.51$; $d_p = 2.6$ mm ; $\rho_p = 1140$ kg.m^{-3} ; $\mu_2 = 0.7$; $I_0 = 0.3$ and $\kappa = 0.35$

- Good overall agreement in velocity profiles (discrepancy $\leftrightarrow$ turbulence model)
- Similar concentration profiles obtained with phenomenological model and kinetic theory$\longrightarrow$ both exhibit a concentration shoulder

Solid load comparison with literature data

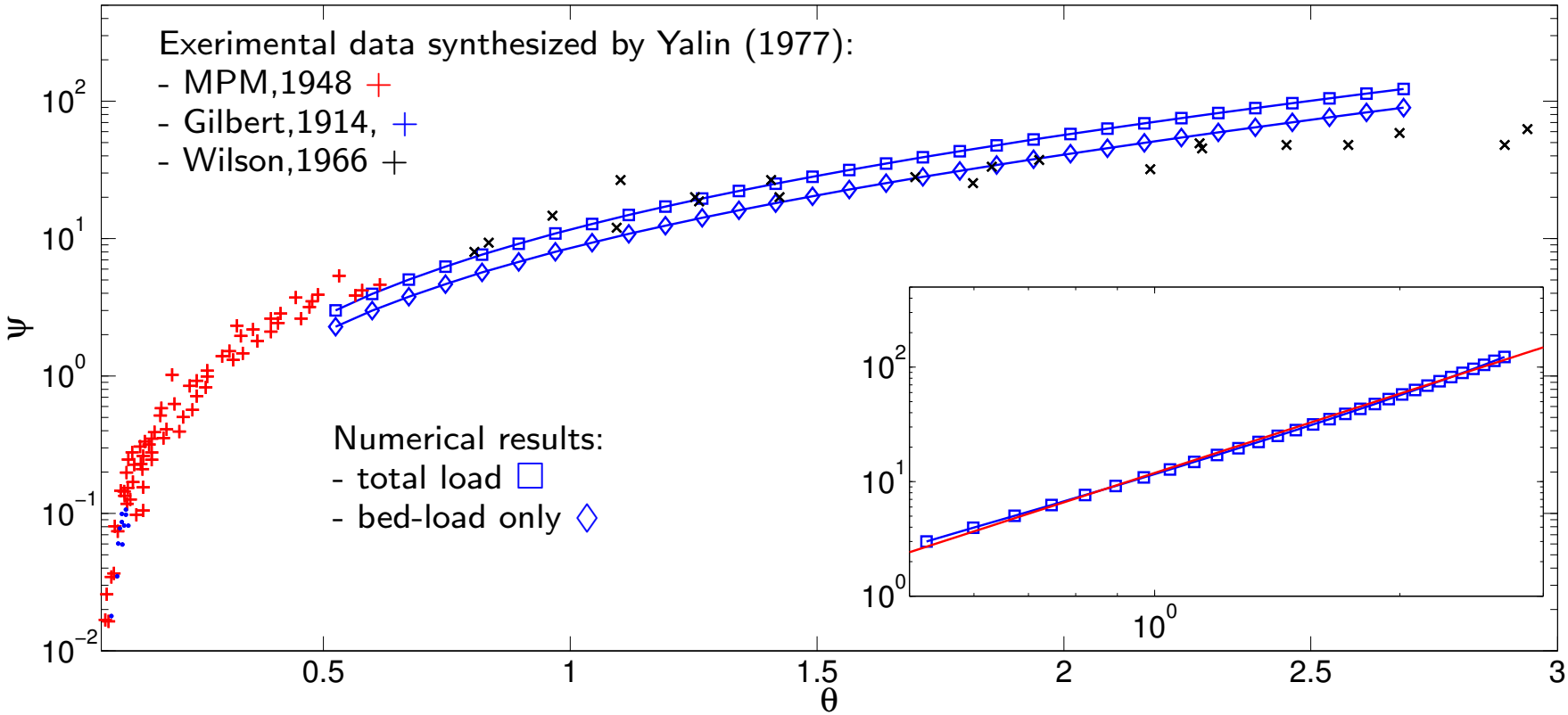

Fig. : Dimensionless sediment transport rate $\psi = q_p/\rho_p\sqrt{(\rho_p - \rho_f)gd_p^3/\rho_f}$ and SBL contribution $\psi^{SBL} = q_p^{SBL}/\rho_p\sqrt{\rho_p g d_p^3/\rho_f}$ versus Shields parameter θ.

- Good predictions of solid load on a large range of Shields numbers $\theta \in [0.5; 2.5]$
- Power law predicted by the model: $\psi = 11.9\ \theta^{2.3}$

Comparison with Sumer *et al.* experiments: sheet layer thickness

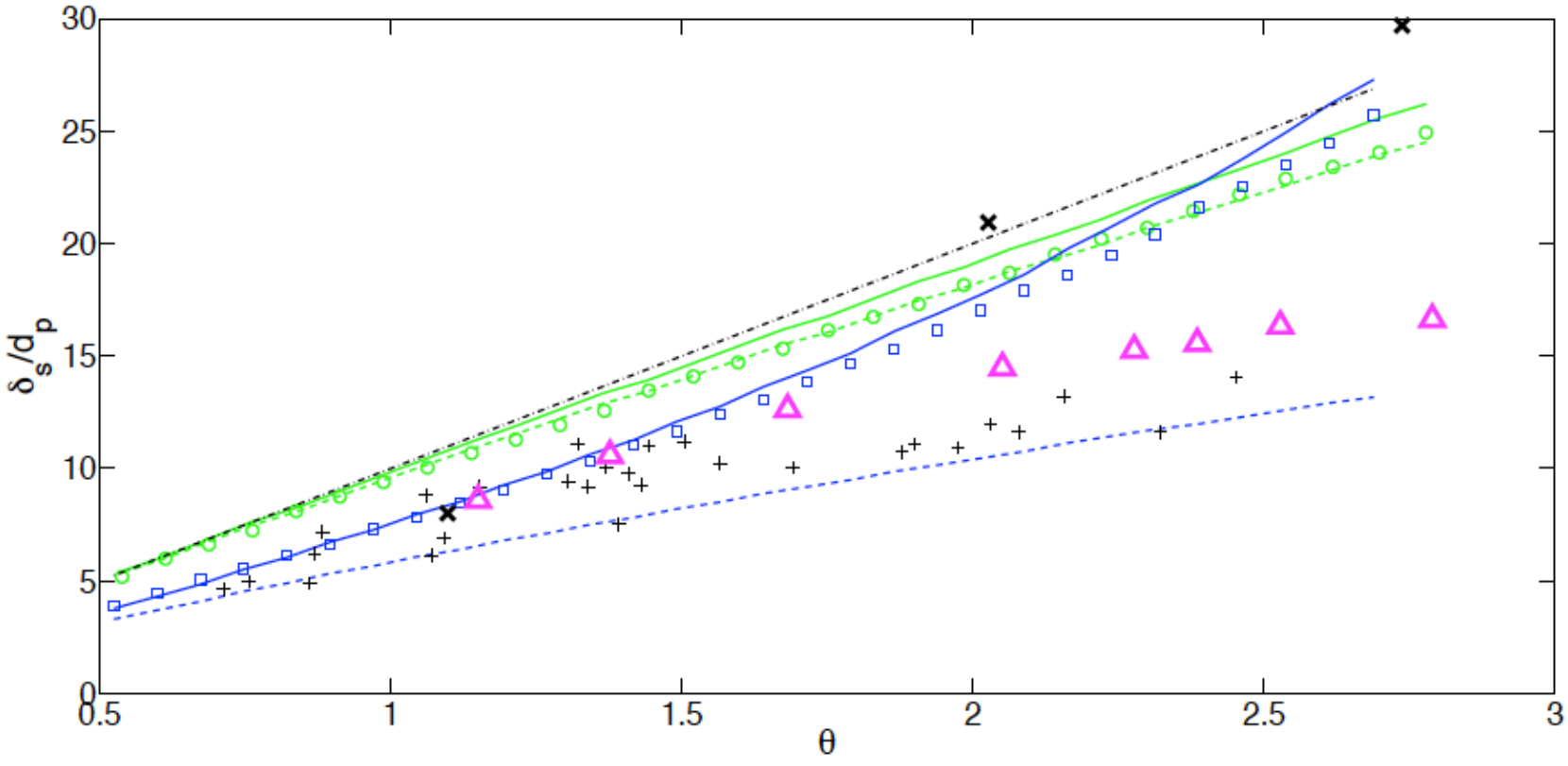

Figure 7. Comparison of the dimensionless sheet flow layer thickness $\delta_s/d_p = (h_p - h_c)/d_p$ between the present model results for sediment types A: numerical solution (□), equation (32) (——), equation (33) (- - -), and B: numerical solution (○), equation (32) (——), equation (33) (- - -), model results from *Hsu et al.* [2004] (△), *Wilson* [1987]'s model predictions (- . -) and *Sumer et al.* [1996]'s data from visual observations (+) and from concentration profiles (x).

$$\frac{\delta_s}{d_p} = \frac{\theta}{\mu_s\ \bar{\phi}\ \cos\beta - \left[\rho_f/(\rho_p - \rho_f) + \bar{\phi}\right]\sin\beta} \qquad (32)$$

$$\frac{\delta_s}{d_p} = \frac{\theta}{\mu_s \bar{\phi}} \qquad (33)$$

Comparison with Sumer *et al.* experiments: Flux and stresses repartition

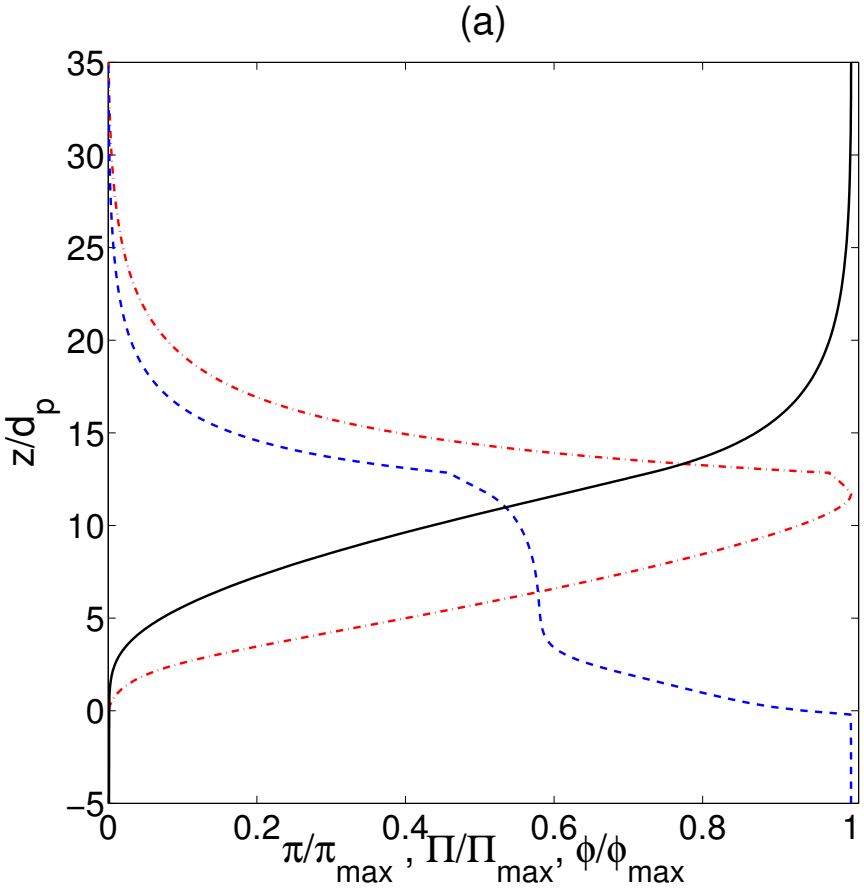

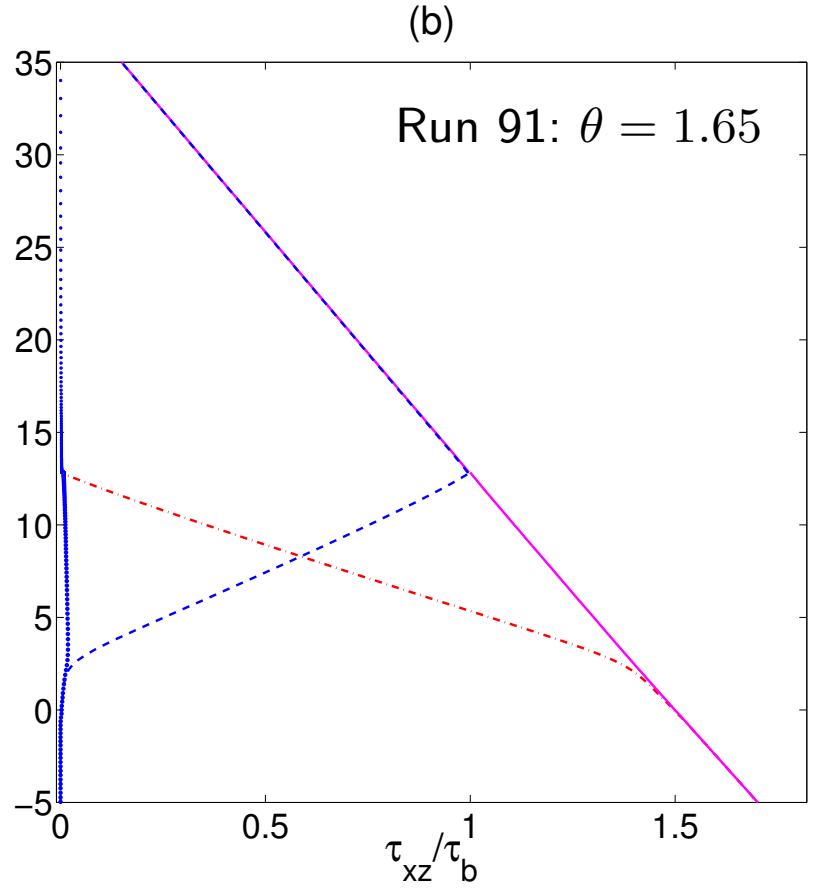

Concentration profile (- - -)

Local volume flux (-·-): $\pi(z) = \phi(z)u^p(z)$

Cumulative flux (—): $\Pi(z) = \int_0^z \phi(\xi)u^p(\xi)d\xi$

- Effective viscous stresses are negligible
- Sheet layer divided into two parts:

  upper $\leftrightarrow$ turbulence

  lower $\leftrightarrow$ intergranular interactions

Experiments: Unidirectional, quasi-Uniform and quasi-Steady sheet flow

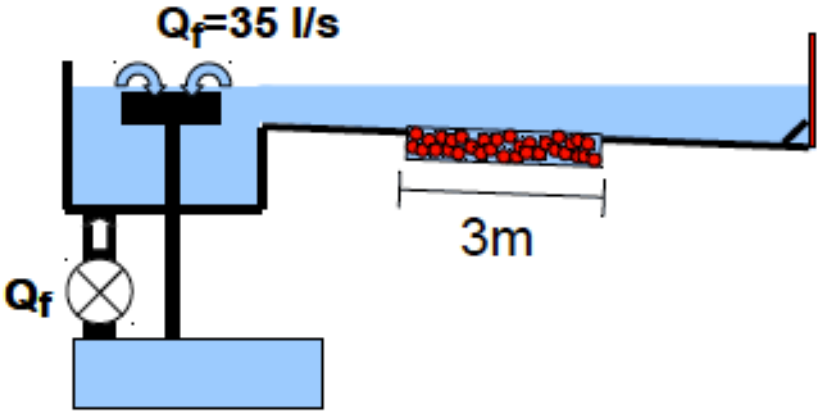

T=0

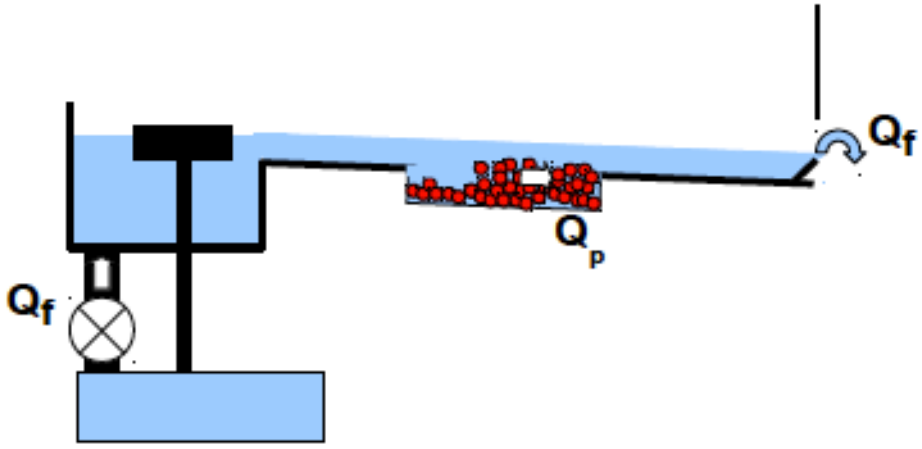

T>0

Parameters:

$L = 10$m $\quad Q_f = 35$ L/s
$W = 0.35$m $\quad S = 0.5\%$
$H_f \approx 0.1$m

PMMA particles
$\rho_p = 1192\ kg/m^3$
d_{50} =3 mm
$\mu_s = \tan(35°) \approx 0.7$

Measurement devices:

- HighSpeed Camera (max 300 Hz)
- Acoustic Doppler profilers:
  - Vectrino II (Nortek):
    $f = 10$ MHz
    $H_{meas} = 3$cm
    $\Delta z = 1$ mm / $f_{acq} = 100$ Hz
  - ADVP :
    $f = 1.25$ MHz
    $H_{meas} = 20$cm
    $\Delta z = 3$ mm / $f_{acq} = 30$ Hz

Experiments: Unidirectional, quasi-Uniform and quasi-Steady sheet flow

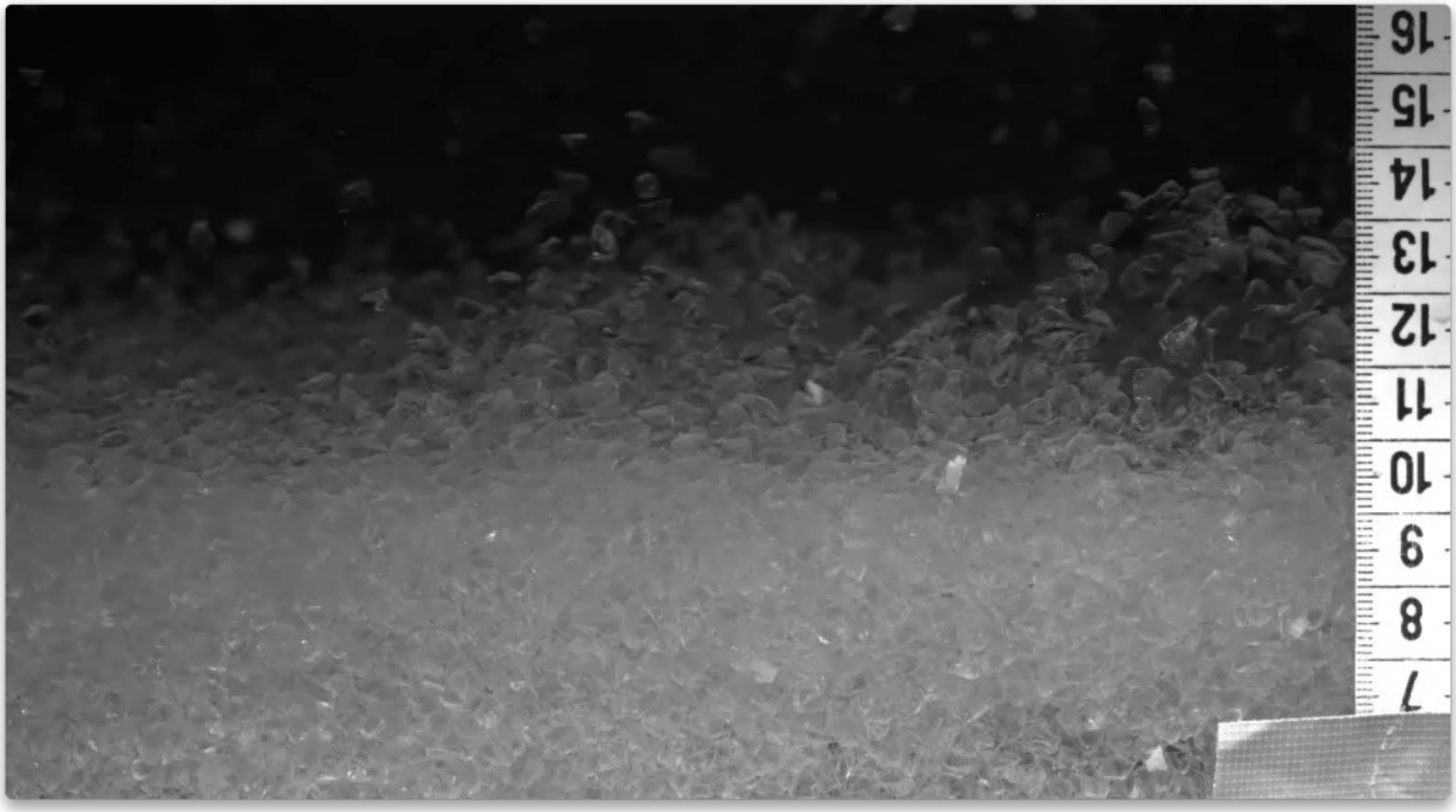

Dimensionless numbers:

$\theta \approx 0.5 - 0.6$

$Re = \dfrac{U\ H_f}{\nu_f} \approx 10^5$

$Re_p = \dfrac{w_s\ d_p}{\nu_f} \approx 2.10^2$

$\dfrac{w_s}{u_*} = 1.4$ (no suspension)

$St = \dfrac{\tau_p}{\tau_f} \approx 25$ with $\tau_f = \dfrac{\nu_f}{u_*^2}$

with $\tau_p = \dfrac{w_s}{g}$

Experimental set-up

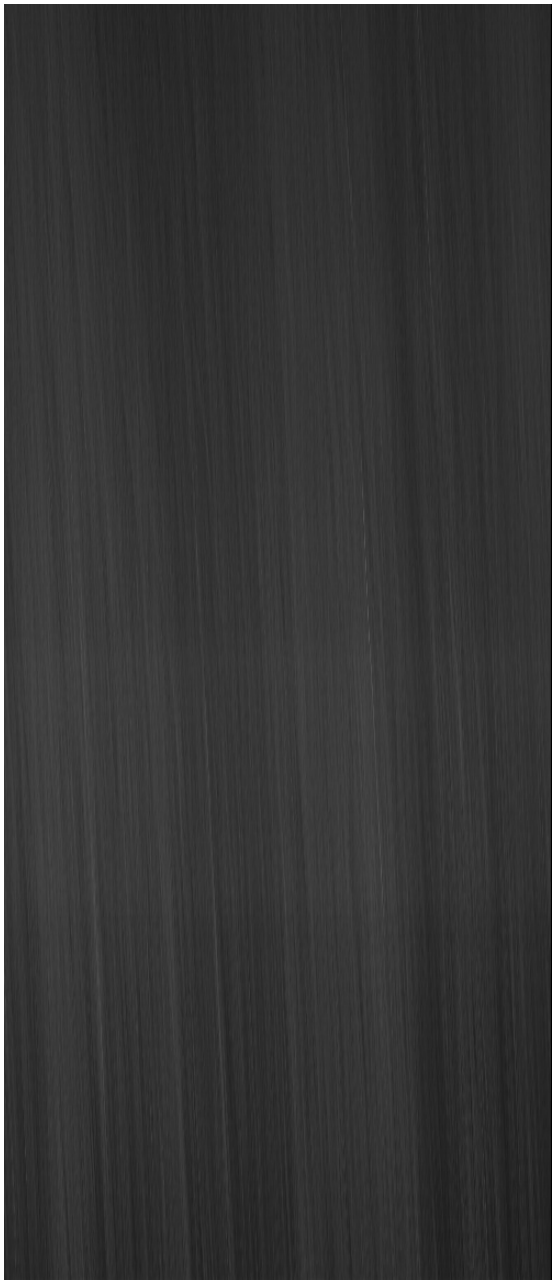

- The same experiment is repeated 10 times
- Upper and lower interface positions are deduced from greylevel threshold on the images
- Lower interface position can also be deduced from acoustic measurement
- Velocity profiles are obtained from two different acoustic doppler profilers and space-time correlation method on the images

Space-time correlation:

Time stack of horizontal ROI (1 dp thick)

slope = mean velocity $\rightarrow$ example on the left

(collaboration with P. Snabre, University of Bordeaux, France)

Experimental results: interfaces

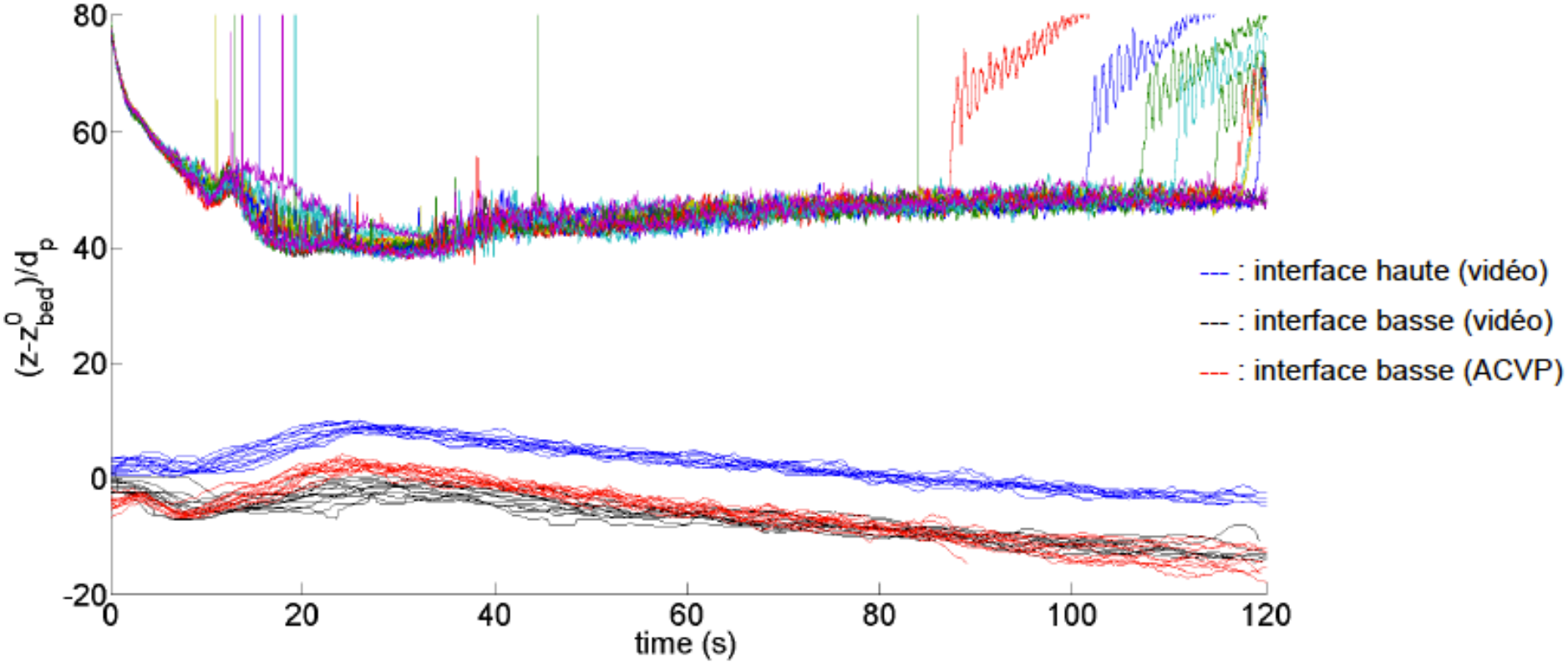

- The same experiment is repeated 10 times
- Upper and lower interface positions are deduced from greylevel threshold on the images
- Lower interface position can also be deduced from acoustic measurement

Experimental results: interfaces

Ensemble averaged experiment:

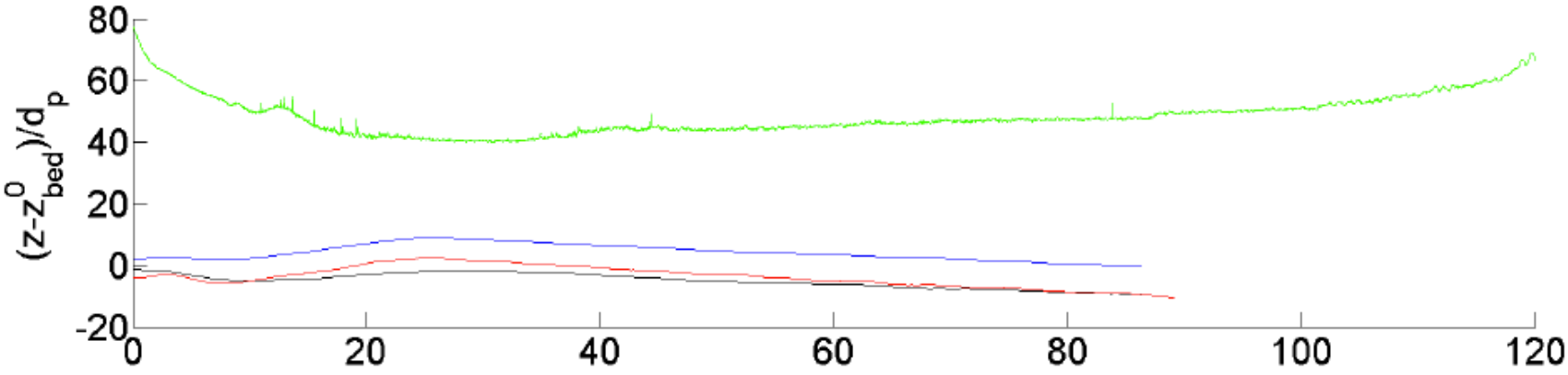

Standard deviation:

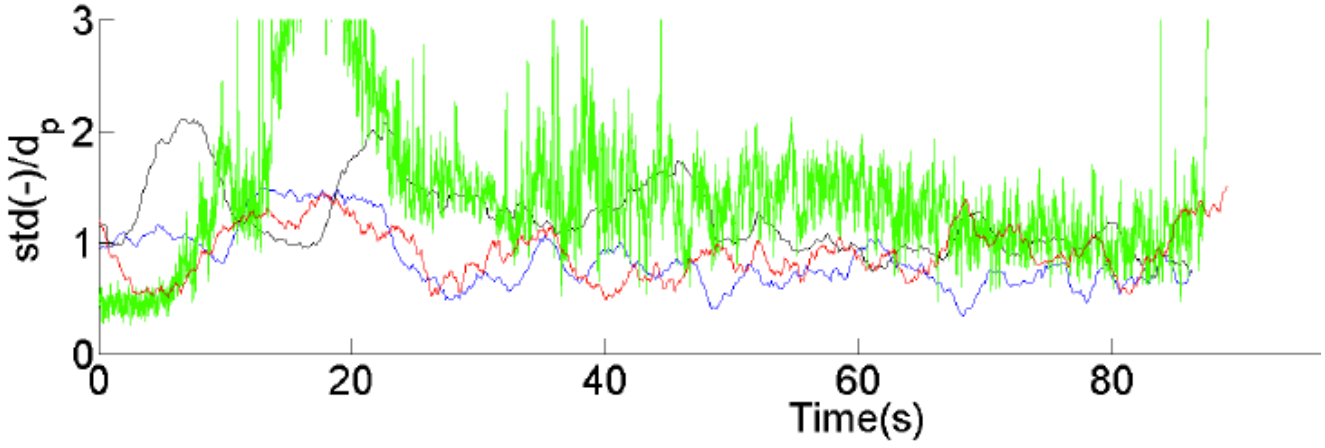

$\longrightarrow$ Experiments are reproducible

Experimental results

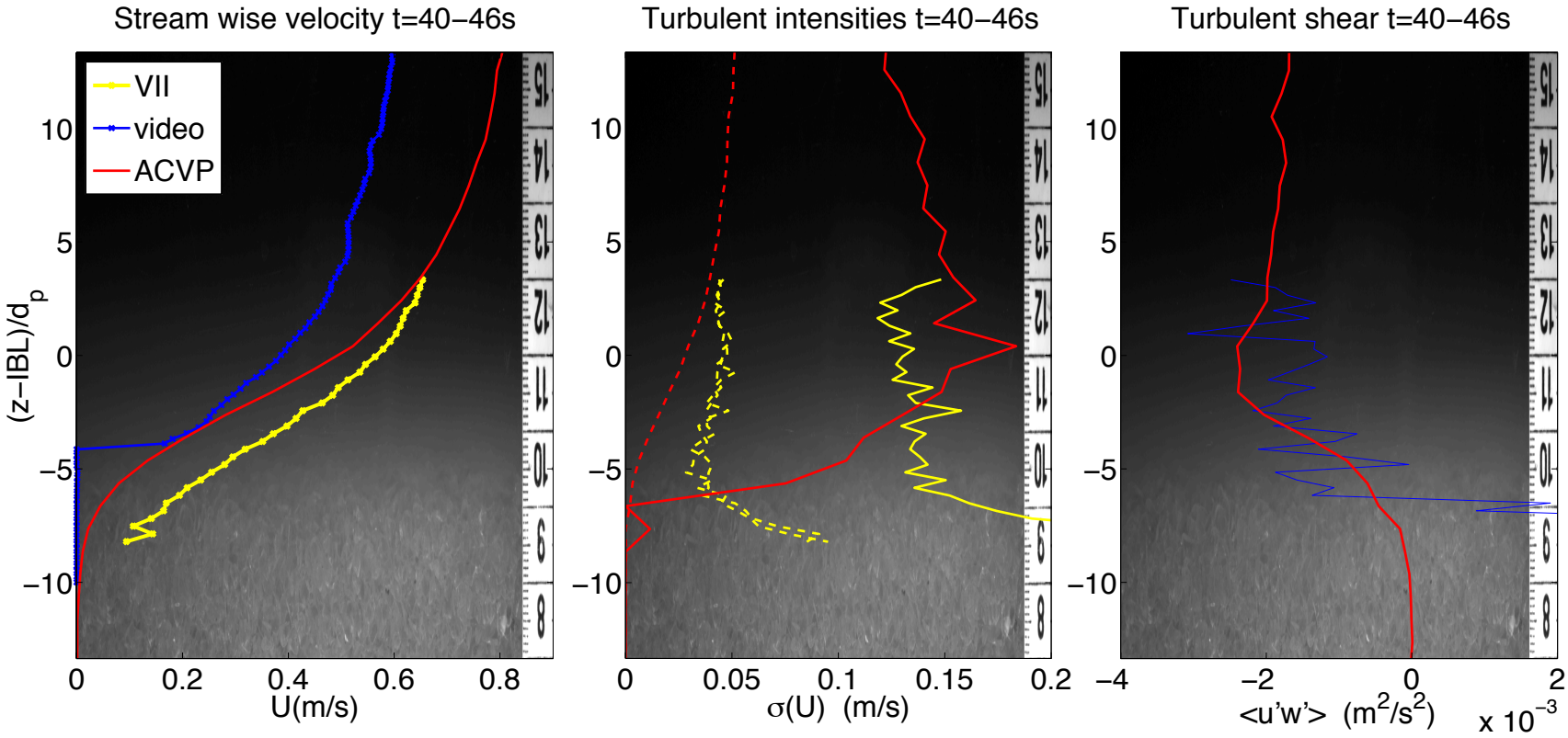

- Acoustic Doppler profilers recovers the same velocity at the top of the sheet flow layer
- Velocity profile deduced from the digital images is much lower than the acoustic ones
  $\rightarrow$ particles velocity (video) is smaller than the fluid velocity (acoustic doppler)
- Turbulent quantities are not converged with the vectrino II (not enough statistics)

Quadrant analyses: Moving bed Vs Fixed bed

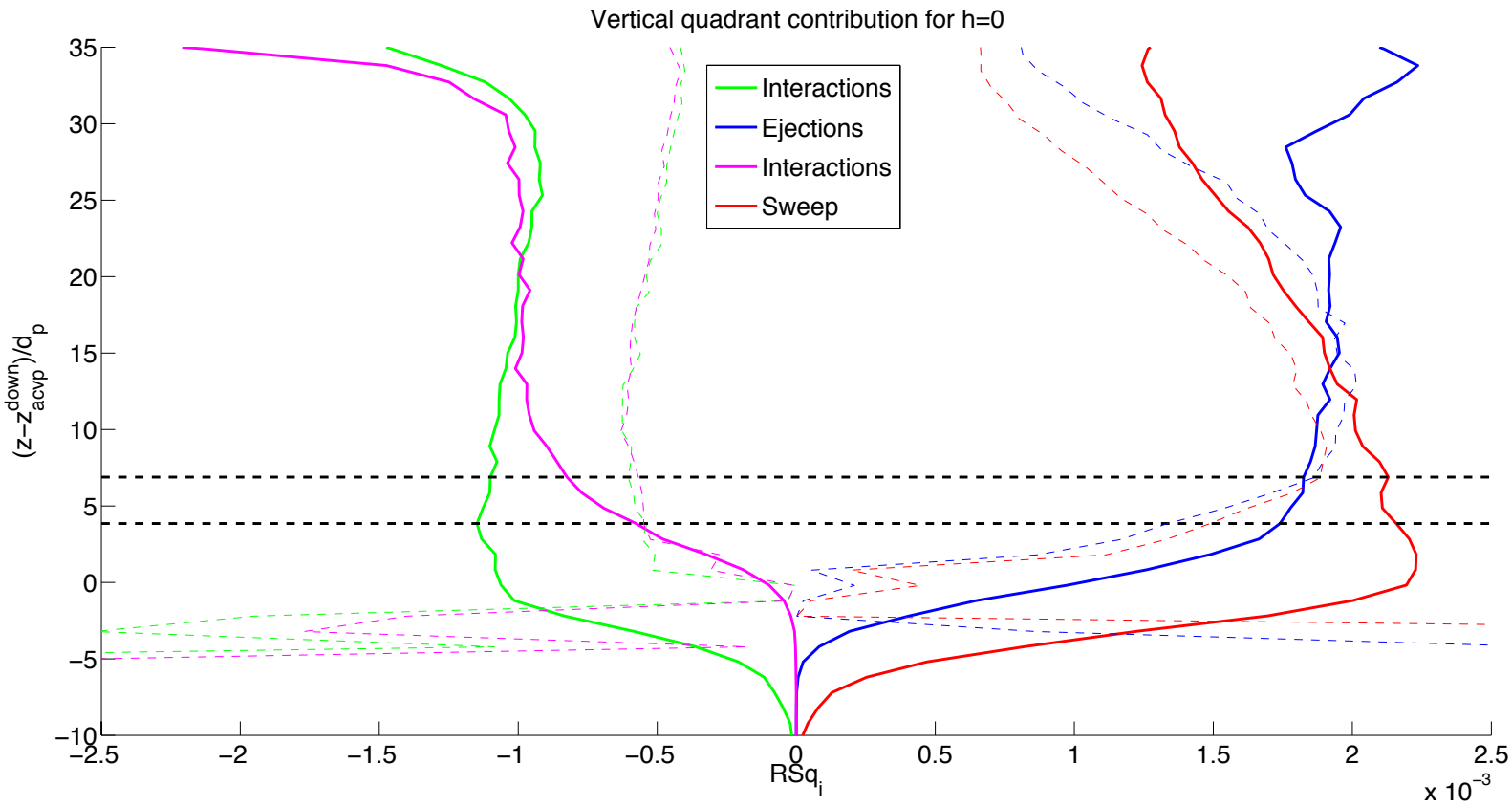

- Sheet layer: Sweeps > Burst // Fixed bed: Sweeps ≈ Bursts
- Crossing between Sweeps & Burst occurs higher under sheet flow conditions
- Interactions are two times larger than in the fixed bed case

Logarithmic profile: Fixed bed experiments

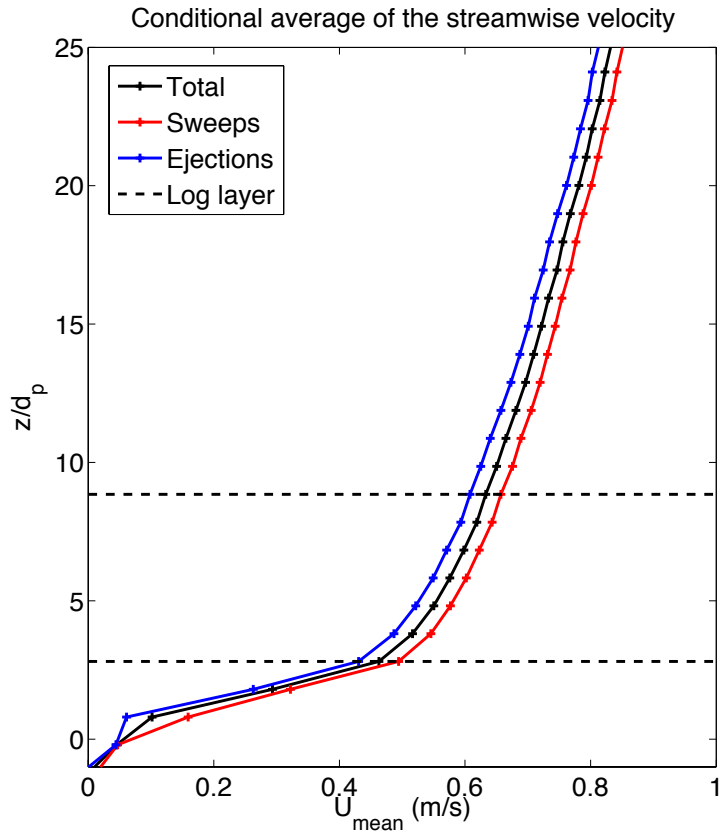

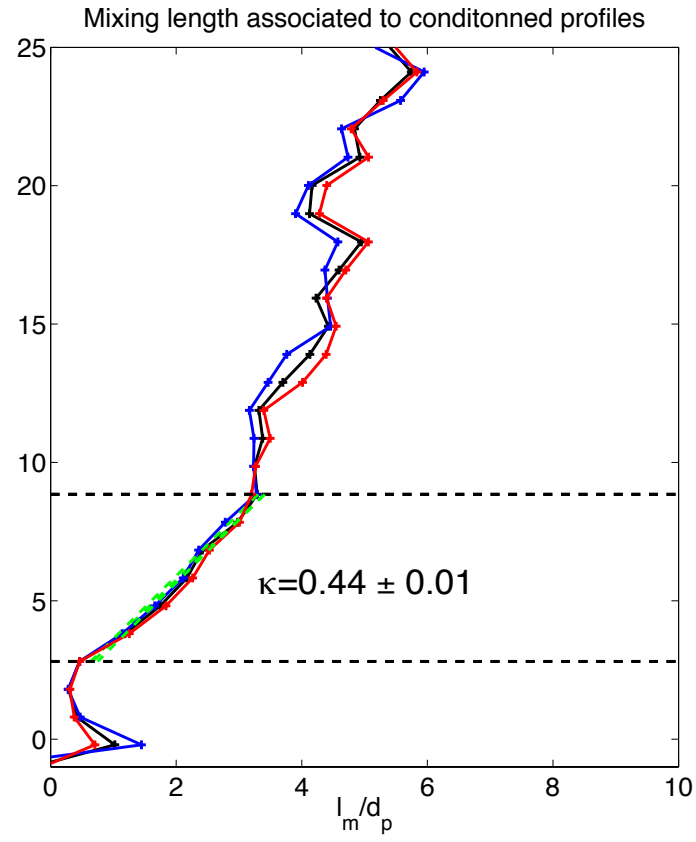

Logarithmic profile: $\dfrac{\partial U}{\partial z} = \dot{\gamma} = \dfrac{u_*}{l_m}$ with $l_m = \kappa z$

u_* is deduced from Reynolds shear stress measurements

$\dot{\gamma}$ is deduced from mean velocity profile

If a log layer exists $\dot{\gamma}$ should be linear in $z \Rightarrow \kappa = \dfrac{u_* \dot{\gamma}^{-1}}{z}$ =constante

Logarithmic profile: Moving bed experiments (acoustic measurements)

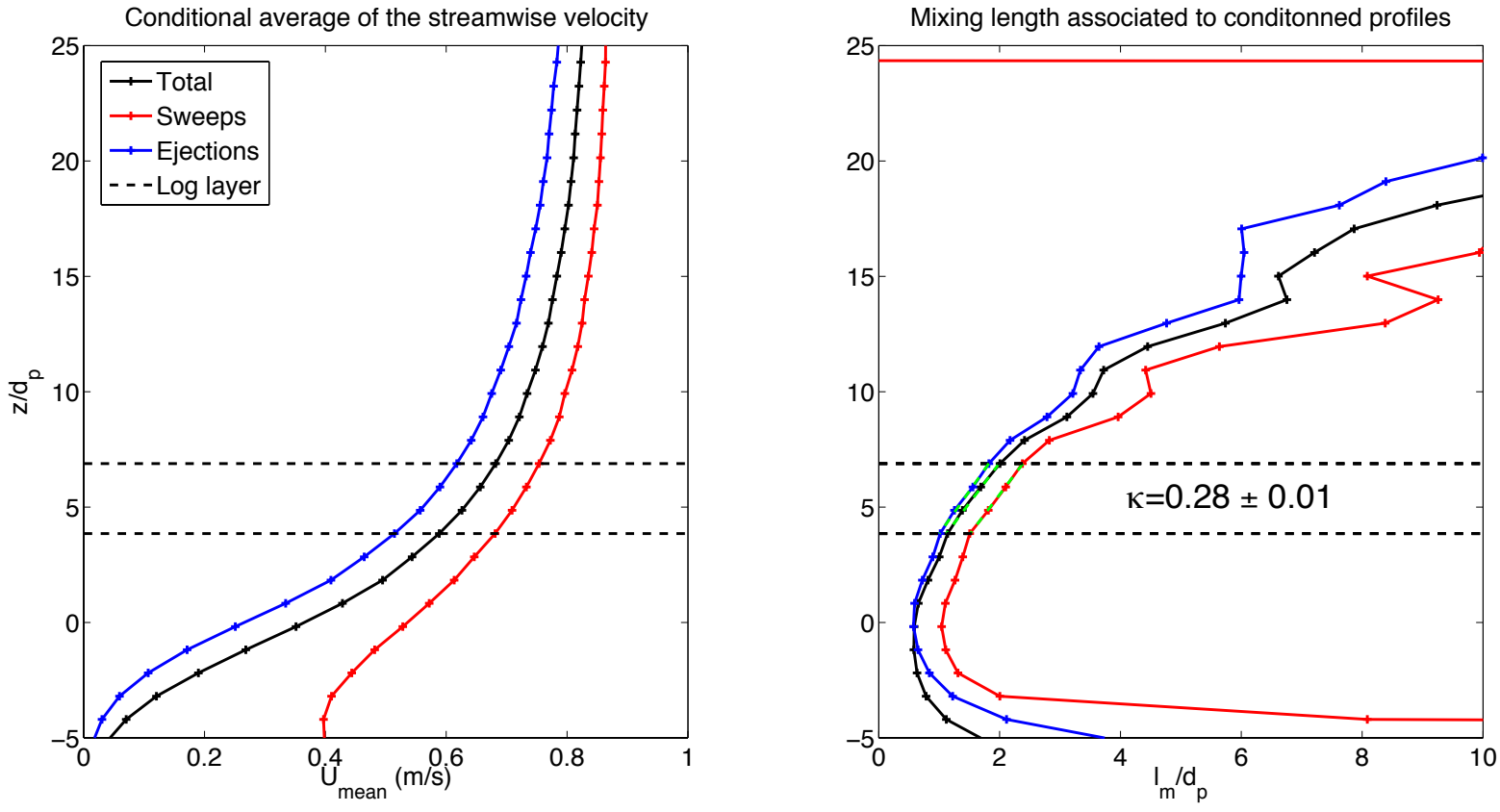

A log layer is still observed: $\kappa = 0.28$ (lower than in clear water)

Logarithmic profile: Moving bed experiments (video measurements)

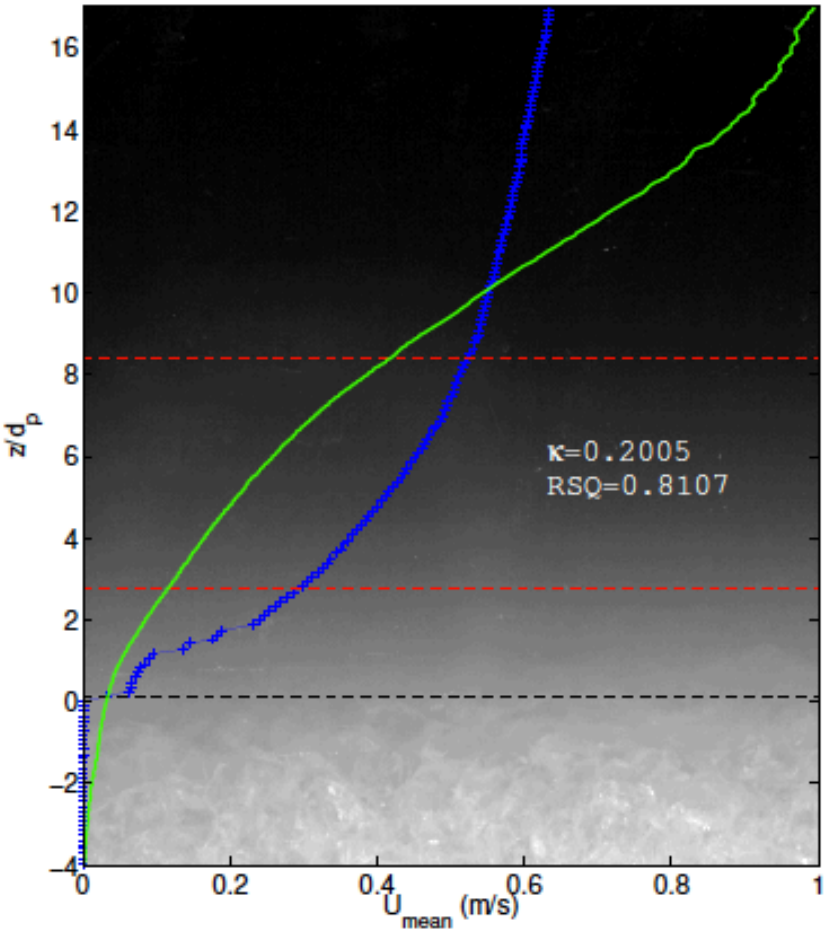

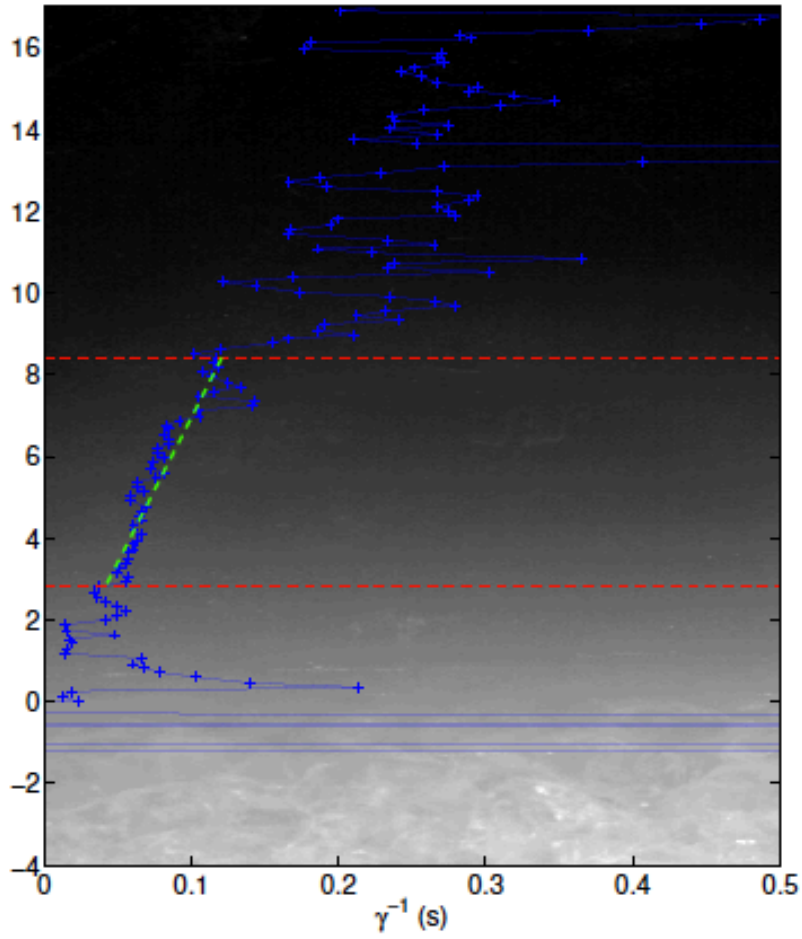

A log layer is again observed with $\kappa \approx 0.2 \Rightarrow \kappa = \dfrac{\kappa_{CW}}{2}$

Density stratification?

Gradient Richardson number: $Ri = \dfrac{g\dfrac{\partial \rho}{\partial z}}{\rho\left(\dfrac{\partial u}{\partial z}\right)^2}$

Rough estimates:

- $\delta \approx 5 - 10\ d_p$
- $U_{max} \approx 0.4 - 0.6$ m/s
- $\overline{\phi} = \dfrac{\phi_{max}}{2}$

$$Ri = \frac{g\delta\phi_{max}\Delta\rho}{\left(\rho_f + \overline{\phi}\Delta\rho\right)U_{max}^2} \approx 0.1$$

Does density stratification is responsible for the damping of turbulence through the sheet-flow layer?

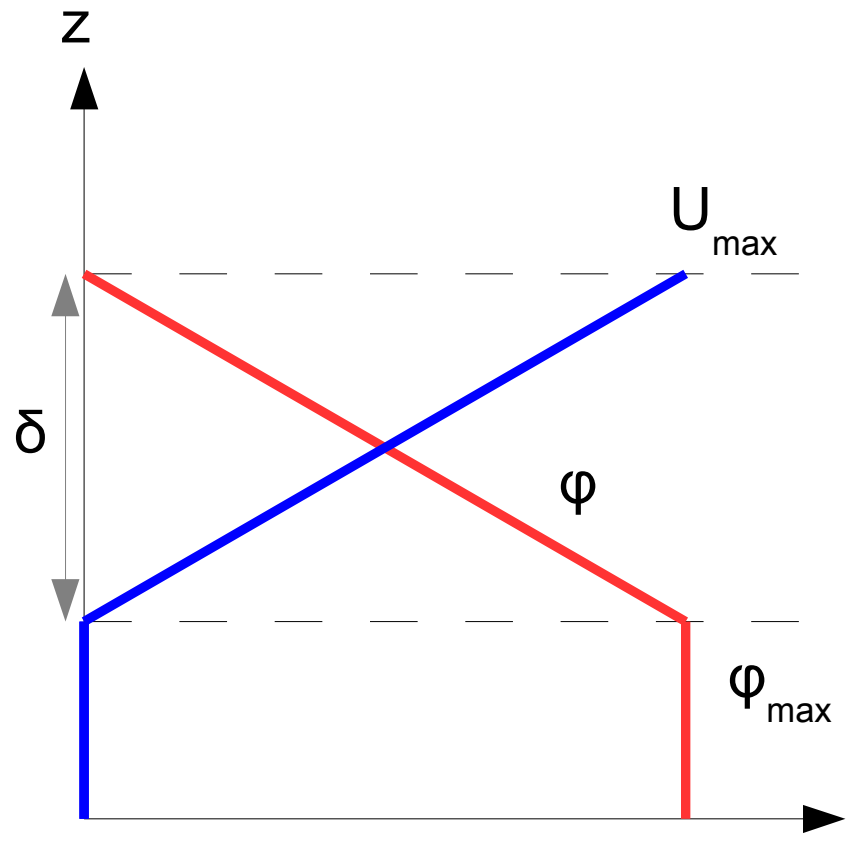

Conclusions

- Dense granular rheology can be used to describe intergranular stresses in sheet-flow
- First turbulence measurements down to the fixed bed has been obtained under sheet flow conditions

On-going work

- Improve the sheet-flow model by accounting for turbulent dispersion inside the "sediment bed layer"
- Implementation in a 3D numerical model...
- Analysis of the measurements to understand why the turbulent structures are so strongly modified by the presence of a movable bed
- Experiments with spherical particles and smaller particles (non-spherical) *i.e* non-massive particles $w_s/u_* < 1$

1. Introduction

2. Laminar bed-load
   - Experiments:Index-matching technique
   - Modeling approaches:Two-phase model
   - Model data comparisons

3. Sheet-flow of massive particles
   - Modeling approach
   - Validation and comparison with literature data
   - Sheet-flow experiments at LEGI

4. Conclusions and on-going work

Summary

- Dense granular rheology can be used to describe intense bed-load transport (laminar and turbulent)
- Regularization technique can be used to implement this rheology in 3D numerical model
- First turbulence measurements down to the fixed bed has been obtained under sheet flow conditions

Open questions

- Does the buoyancy plays a role in the dense granular rheology ?
- What happens to the turbulence at the transition between the dilute suspension and the dense static bed ? How can we model it ?

Plane shear experiments: Dimensional analysis (1/2)

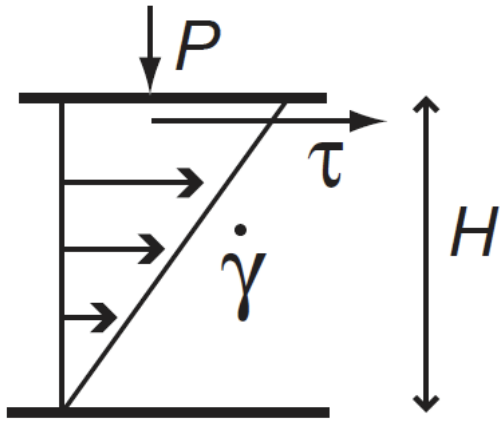

- Monodisperse spherical particles with density ρ_p and diameter d
- Imposed pressure P and velocity V on the top plate $\Rightarrow \dot{\gamma} = \dfrac{V}{H}$.
- Measure the shear stress τ that develops on the top plate

For large system ($H >> d$) a single dimensionless number control the system:

$$\text{Inertial number: } I = \frac{\dot{\gamma}\, d}{\sqrt{P/\rho_p}}$$

Da Cruz et al. (2004), Lois et al. (2005)

Plane shear experiments: Dimensional analysis (2/2)

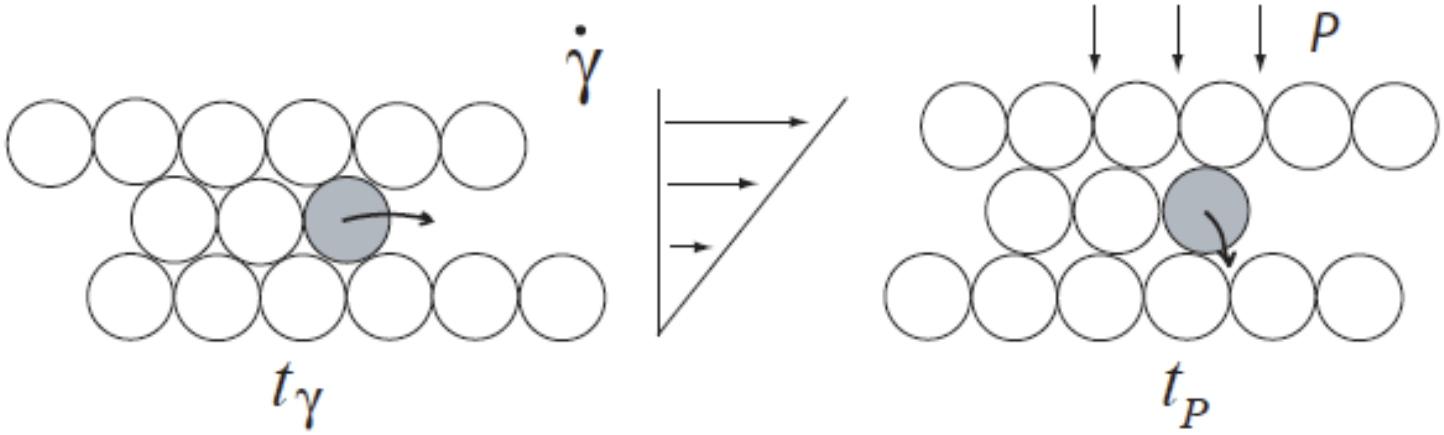

Andreotti, Forterre and Pouliquen (2011)

Interpretation of the Inertial number:

$$I = \frac{\dot{\gamma}\, d}{\sqrt{P/\rho_p}} = \frac{t_{micro}}{t_{macro}} \quad where \quad t_{micro} = \frac{d}{\sqrt{P\ /\ \rho_p}} \ and \ t_{macro} = \frac{1}{\dot{\gamma}}$$

Da Cruz et al. (2004), Lois et al. (2005)

The shear stress is proportional to the pressure and depends on I, also the volume fraction depends on I:

$$\boxed{\tau = \mu(I)\ P \quad and \quad \phi = \phi(I)}$$

Local rheology: dry granular flows / inertial regime

The following curves are obtained from experiments and tends to confirm the previous postulated constitutive laws

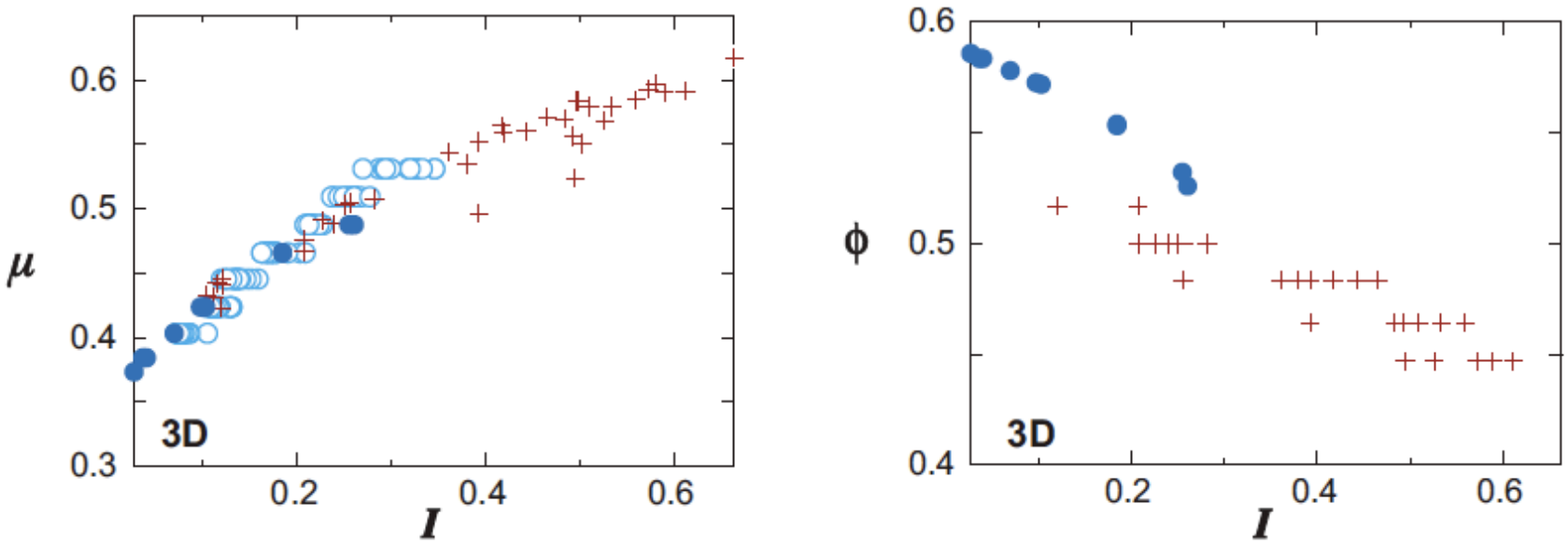

GDR Midi (2004), Pouliquen (1999), Baran et al. (2006), Savage and Sayed (1984) from Forterre and Pouliquen (2008)

Functions can be fitted to these data in order to get explicit relationship for the constitutive laws:

$$\mu(I) = \mu_s + \frac{\mu_2 - \mu_s}{I_0/I + 1} \quad and \quad \phi(I) = \phi_{max} + (\phi_{min} - \phi_{max})\ I$$

with typical values for monodisperse glass beads:

$$\mu_s = tan(21^\circ)\ ;\ \mu_2 = tan(33^\circ))\ ;\ I_0 = 0.3\ ;\ \phi_{max} = 0.6\ and\ \phi_{min} = 0.4$$

Two-phase equations

Horizontal momentum equations:

$$0 = \frac{\mathrm{d}\tau^f_{xz}}{\mathrm{d}z} + \frac{\mathrm{d}R^f_{xz}}{\mathrm{d}z} - nf_x + \epsilon\ \rho_f\ g\ \sin\beta$$

$$0 = \frac{\mathrm{d}\tau^p_{xz}}{\mathrm{d}z} + nf_x + \phi\ \rho_p\ g\ \sin\beta$$

Generalized buoyancy and drag force: $nf_x = \phi\frac{d\tau^f_{xz}}{dz} + C_D\ (U - u^p)$

$$0 = \frac{\mathrm{d}R^f_{xz}}{\mathrm{d}z} + \epsilon\frac{\mathrm{d}\tau^f_{xz}}{\mathrm{d}z} - C_D\ (U - u^p) + \epsilon\ \rho_f\ g\ \sin\beta$$

$$0 = \frac{\mathrm{d}\tau^p_{xz}}{\mathrm{d}z} + \phi\frac{\mathrm{d}\tau^f_{xz}}{\mathrm{d}z} + C_D\ (U - u^p) + \phi\ \rho_p\ g\ \sin\beta$$

where C_D is given by: $C_D = \frac{\rho_f\ \phi}{d_p\ (1-\phi)^{3.1}}\left(0.3\ (U - u^p) + 18.3\ \frac{\eta_f}{\rho_f\ d_p}\right)$

Dallavalle (1943) + Richardson and Zaki (1954)

Closure issue: relate τ^f_{xz}, R^f_{xz} and τ^p_{xz} to averaged quantities